REPORT No. 642

TESTS OF FIVE FULL-SCALE PROPELLERS IN THE PRESENCE OF A RADIAL AND A LIQUID-COOLED ENGINE NACELLE, INCLUDING TESTS OF TWO SPINNERS

By David Biermann and Edwin P. Hartman

SUMMARY

Wind-tunnel tests are reported of five 3-blade 10-foot propellers operating in front of a radial and a liquid-cooled engine nacelle. The range of blade angles investigated extended from 15° to 45°. Two spinners were tested in conjunction with the liquid-cooled engine nacelle. Comparisons are made between propellers having different blade-shank shapes, blades of different thickness, and different airfoil sections.

The results show that propellers operating in front of the liquid-cooled engine nacelle had higher take-off efficiencies than when operating in front of the radial engine nacelle; the peak efficiency was higher only when spinners were employed. One spinner increased the propulsive efficiency of the liquid-cooled unit 6 percent for the highest blade-angle setting investigated and less for lower blade angles. The propeller having airfoil sections extending into the hub was superior to one having round blade shanks. The thick propeller having a Clark Y section had a higher take-off efficiency than the thinner one, but its maximum efficiency was possibly lower. Of the three blade sections tested, Clark Y, R. A. F. 6, and N. A. C. A. 2400–34, the Clark Y was superior for the high-speed condition, but the R. A. F. 6 excelled for the take-off condition.

INTRODUCTION

A series of tests of full-scale propellers was made in the propeller-research tunnel during the first part of 1937. Published reports of the series cover separate subjects as: compressibility effects (reference 1), solidity (reference 2), negative thrust and torque (reference 3), and blade section (reference 4). The results of tests of five propellers are published in the present report, the purpose of which is twofold: first, to present design data from tests of four 3-blade propellers made in the presence of two popular body types; and, second, from the test data for all five propellers, to make incidental comparisons regarding the effect of: body shape and size, spinners, blade-shank shape, blade thickness, and blade section. The concrete data should be of value in design work because two of the propellers are in fairly wide use and the body types are representative of those in common use. The comparisons may be of value in the determination of some of the elements of the basic design of airplanes and propellers.

APPARATUS AND METHODS

The propeller-research tunnel has been modified since the description of reference 5 was written to the extent of installing an electric motor to drive the tunnel propeller and of replacing the balance with a more modern one capable of simultaneously recording all the forces.

A 600-horsepower Curtiss Conqueror engine (GIV–1570) was used to drive the test propellers. The engine

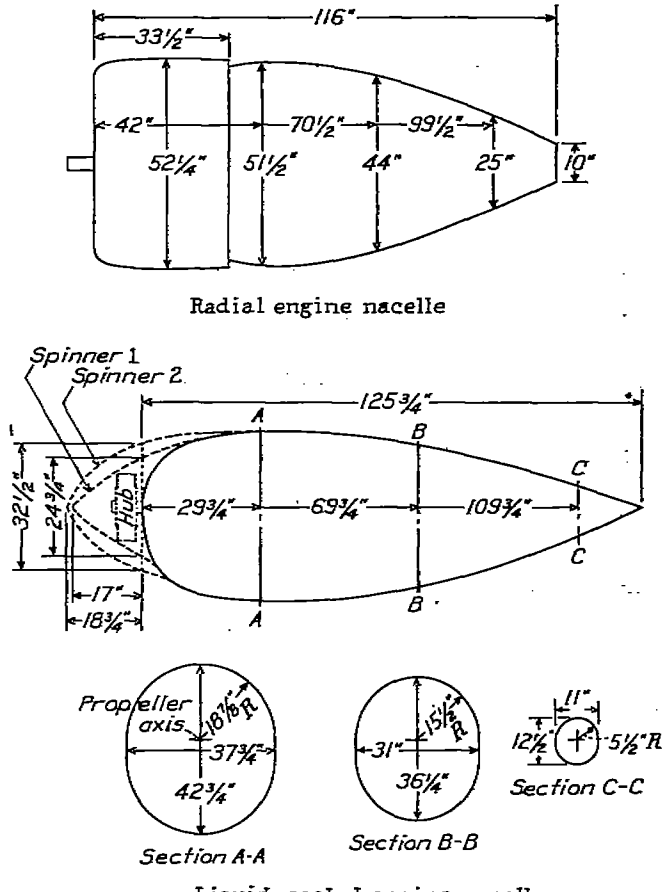

FIGURE 1.—Drawings of engine nacelles.

was mounted in a cradle dynamometer free to rotate about an axis parallel to the propeller axis and located at one side of the engine. The torque reaction was transmitted from the other side of the engine to recording scales located on the floor of the test chamber. The propeller speed was measured by a calibrated electric tachometer.

A scale drawing of each nacelle is given in figure 1.

A perforated plate was used to simulate in air resistance a radial engine in those tests in which the radial engine cowling was used. (See fig. 2.) The cowling was selected because its drag was not sensitive to the propeller slipstream and, consequently, the propulsive efficiency was not abnormally affected. Air was allowed to flow through the plate at a rate corresponding to that for a normally baffled engine. Separate tests to determine the effect on the propeller characteristics of different rates of air flow through the plate indicated that the effect was negligible.

The liquid-cooled engine nacelle was tested with three nose conditions: a round nose, which was the standard condition for nearly all the tests, and with two spinners of different size. The nacelle with the round nose is shown in figure 3 and with spinner 1 in figure 4. An effort was made to reduce the drag of the round blade shanks that extended out from spinner 1 by stream-

FIGURE 2.—The radial engine nacelle.

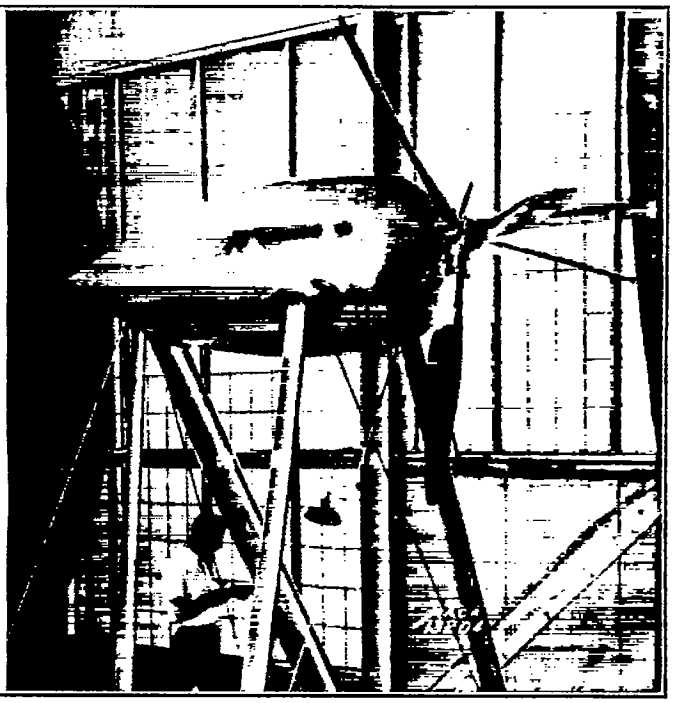

FIGURE 3.—The liquid-cooled engine nacelle with round nose.

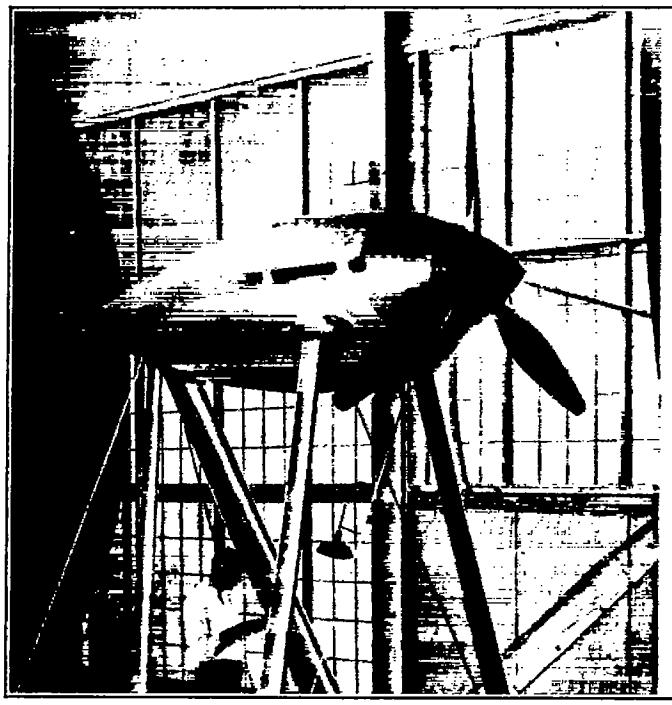

FIGURE 4.—The liquid-cooled engine nacelle with spinner 1.

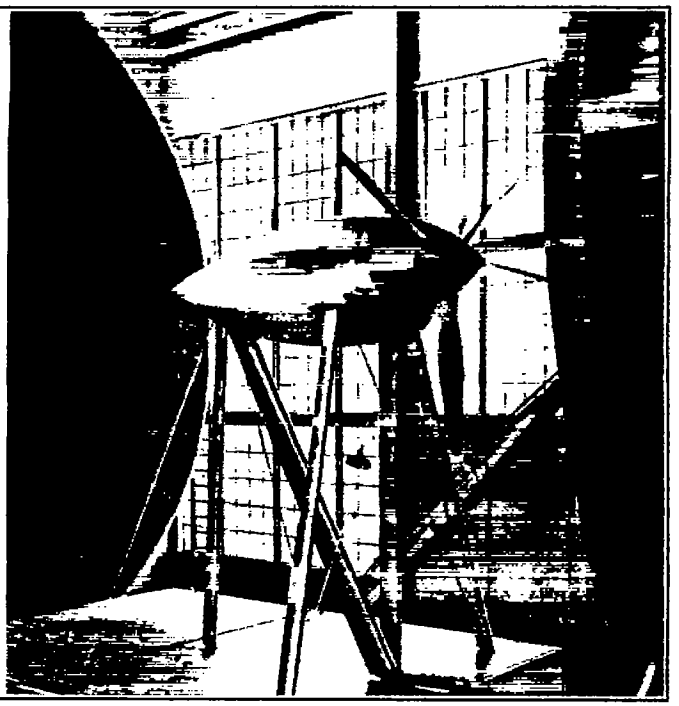

FIGURE 5.—The liquid-cooled engine nacelle with spinner 1 and blade-shank cuffs

lining them with thin sheet-metal cuffs. These cuffs, shown in figure 5, extended along the blade shanks for a distance of about 4 inches beyond the spinner and were secured to the spinner. The blades were thus enclosed for a distance of about 24 percent of the radius.

Five 3-blade propellers (fig. 6), all having diameters of 10 feet, were tested. Blade-form curves are given in figures 7 and 8. The propeller dimensions are given by the following notation: D, diameter; R, radius to the tip; r, station radius; h, section thickness; b, station chord; p, geometric pitch. Figure 9 shows the section outline and gives the ordinates for the three blade sections incorporated in the different propellers. It may be noted that the N. A. C. A. 2400–34 airfoil section is modified for propeller design by changing the thickness with respect to the mean camber line. The camber therefore remains constant for the whole blade, whereas the camber increases with blade section thickness for propellers having the Clark Y and R. A. F. 6 sections.

The principal propeller dimensions are given in the following table:

Propeller drawing number	Diameter (feet)	Section	b/D at $0.75R$	h/b at $0.75R$	Shank shape
Bureau Aeronautics 5868–9.	10	Clark Y	0.061	0.09	Round.
Hamilton Standard 1C1–0	10	do	.059	.07	Airfoil.
[1] Hamilton Standard 6101	10	do	.059	.07	Round.
[1] Hamilton Standard 6129	10	R. A. F. 6	.059	.07	Do.
[1] Hamilton Standard 6131	10	N. A. C. A. 2400–34.	.059	.07	Do.

[1] Controllable.

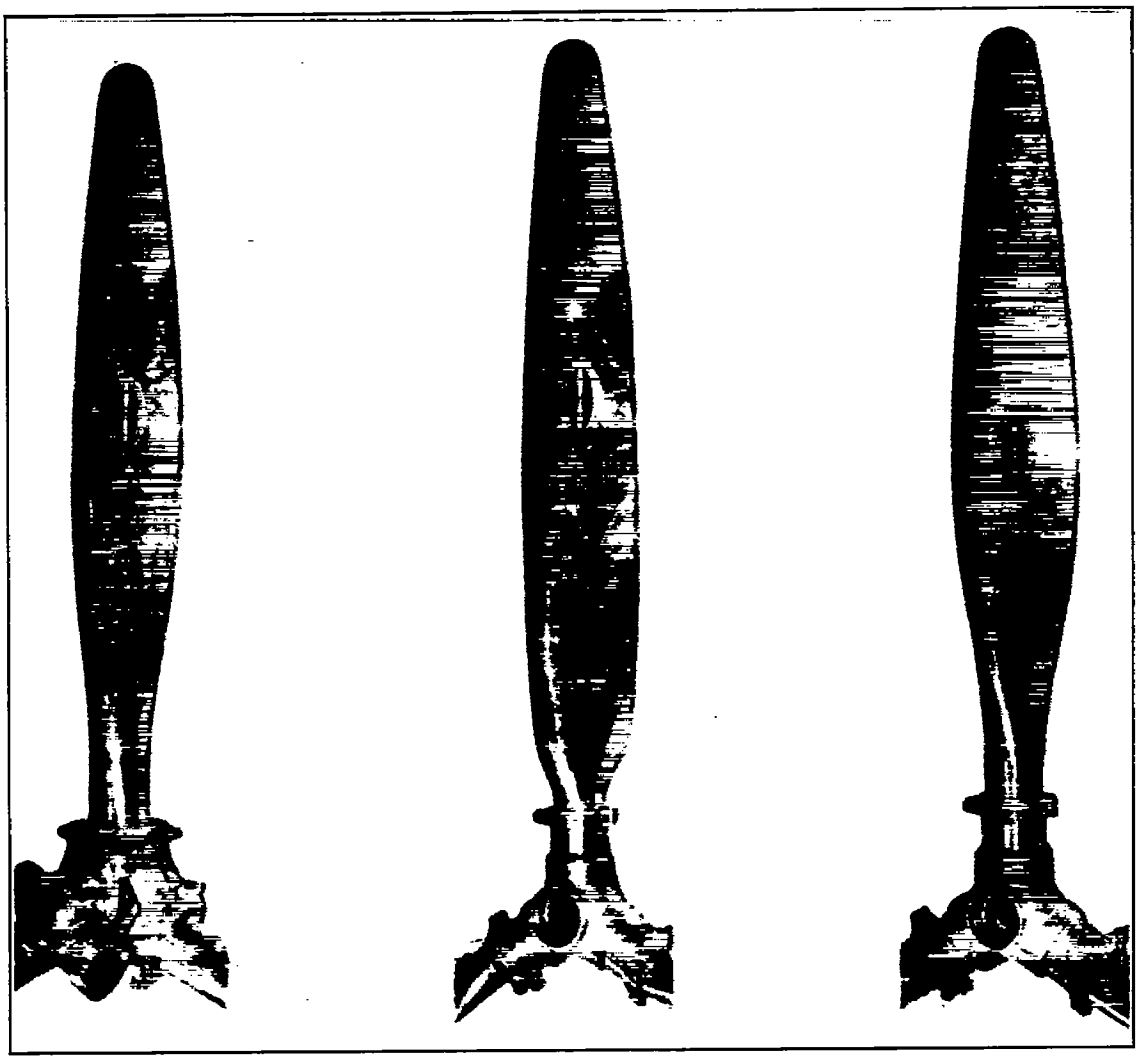

FIGURE 6.—The propeller blades tested.

It may be noted from the table that the essential difference between propellers 5868–9 and 6101 is the blade thickness although propeller 6101 has a slightly larger shank diameter and a different hub, which should not appreciably affect the results. These two propellers probably represent the upper and lower limits in thickness ratios for present-day aluminum-alloy propellers.

Propeller 1C1–0 was included in the series because it differed from 6101 only in the shank shape and, incidentally, in the hub design.

Propellers 6101, 6129, and 6131 constitute a series differing only in blade section. These propellers were whirl-tested (reference 6) and flight-tested at Wright Field previous to the present investigation.

The method of testing in the propeller-research tunnel consists in maintaining the propeller speed constant and increasing the tunnel speed in steps up to the maximum value of 115 miles per hour. Higher values of engine power; the following schedule was therefore adhered to:

Propeller speeds for tunnel speeds below 115 miles per hour

Blade angle, deg.	Initial propeller speed, r. p. m.
15	1,000
20	1,000
25	800
30	800
35	800
40	700
45	700

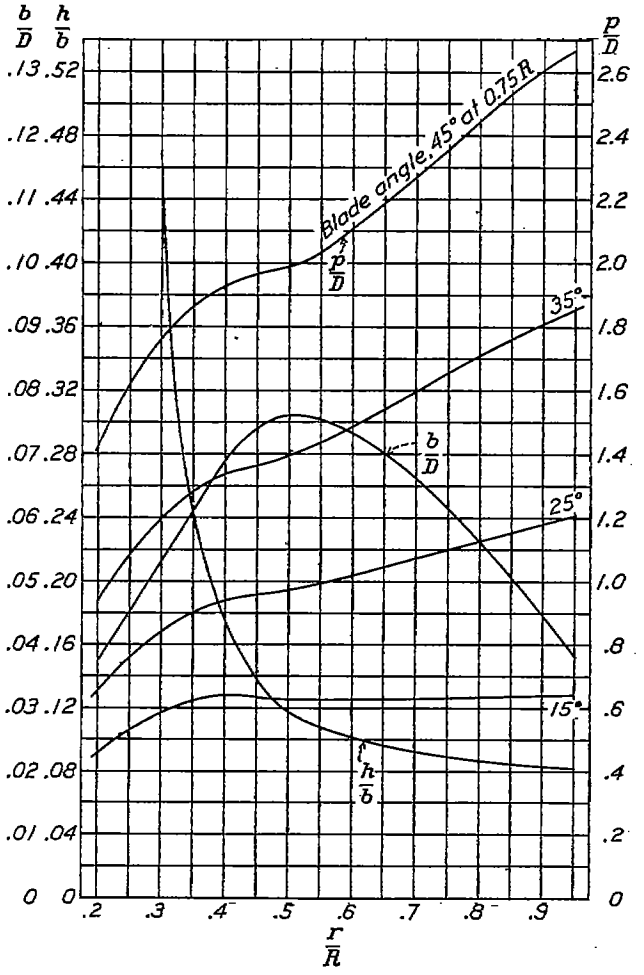

FIGURE 7.—Blade-form curves for propeller 5868-9.

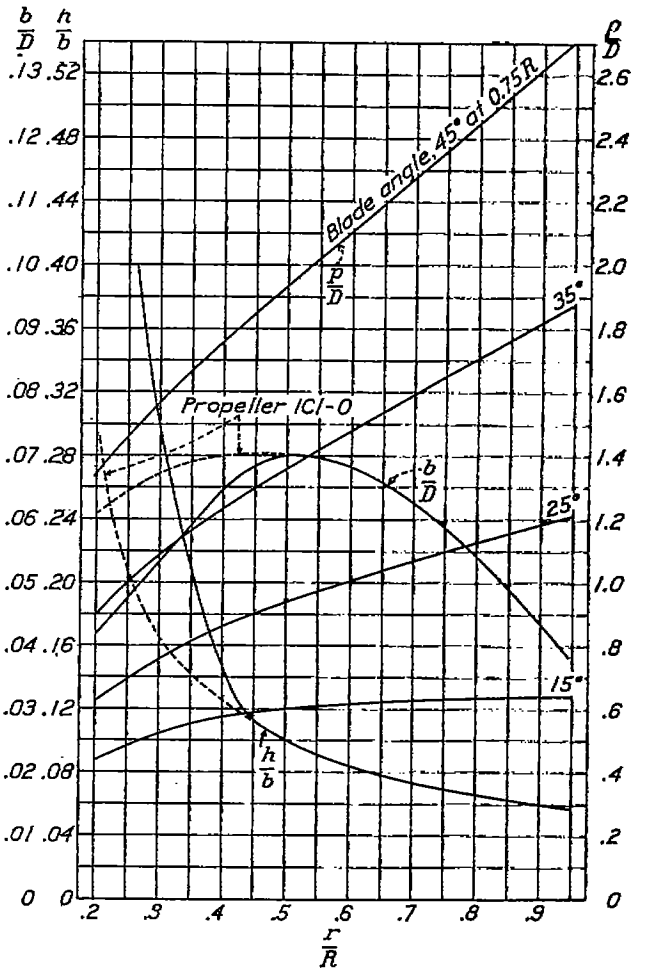

FIGURE 8.—Blade-form curves for propellers 6101, 6129, 6131, and 1C1-0.

of V/nD are obtained by reducing the engine speed until zero thrust is reached.

The tests reported in reference 1 showed that losses in efficiency occurred at tip speeds above 600 to 800 feet per second, depending principally on the blade angle and the V/nD range. At slightly lower tip speeds the values of the thrust and the power coefficients, but not the efficiencies, were affected by compressibility. The present tests were therefore run at tip speeds of 525 feet per second and less to avoid complications arising from compressibility. The standard initial testing propeller speed of 1,000 r. p. m. could not be maintained for the higher blade-angle settings owing to the limitation of

The approximate test propeller speed may be computed from the relation r. p. m.$=\frac{K}{V/nD}$, for V/nD values higher than can be obtained from the foregoing schedule, where $K=1{,}000$ for $V=115$ miles per hour and $D=10$ feet. The tests reported in reference 1 were confined to tip speeds above about 600 feet per second, so the use of the data in this reference for correcting coefficients for normal-flight operating speeds would necessitate neglecting any effects occurring at lower speeds. Unreported data obtained during these tests indicate that this procedure would entail little, if any, error.

RESULTS AND DISCUSSION

The results are reduced to the usual coefficients of thrust, power, and efficiency defined as:

$$C_T=\frac{\text{effective thrust}}{\rho n^2D^4}=\frac{T-\Delta D}{\rho n^2D^4}$$

$$C_P=\frac{\text{engine power}}{\rho n^3D^5}$$

and $$\eta=\frac{C_T}{C_P}\frac{V}{nD}$$

where ρ, the mass density of air.
n, propeller speed.
D, propeller diameter.
ΔD, increased drag of body due to propeller slipstream.

In addition to plots of these coefficients against V/nD, charts for the selection of propellers are given. These charts are based on the speed-power coefficient C_s defined as:

$$C_s=\sqrt[5]{\frac{\rho V^5}{Pn^2}}$$

The test results have been tabulated in ten tables and are available on request from the National Advisory Committee for Aeronautics. The experimental results are presented in chart form in figures 10 to 46. For ease of reference, the figure numbers are listed in the following table:

BASIC DATA

Body	Propeller	Figures
Radial engine nacelle	5868-9	10–13
	6101	14–17
	6129	18–21
	6131	22–25
Liquid-cooled engine nacelle	5868-9	26–29
	6101	30–33
	6129	34–37
	6131	38–41

SPINNER RESULTS AND COMPARISONS

Subject	Propeller	Figure
Spinners	5868-9	42
Blade shank	6101 and 1C1-0	43
Blade thickness	5868-9 and 6101	44
Blade section	6101, 6129, and 6131	45
Body	All propellers	46

BASIC PROPELLER DATA

The chief purpose of this report is to supply propeller data for design purposes. Complete sets of curves of the basic coefficients for each of the propeller-body combinations are given for four propellers, two of which (propellers 5868–9 and 6101) are in common use.

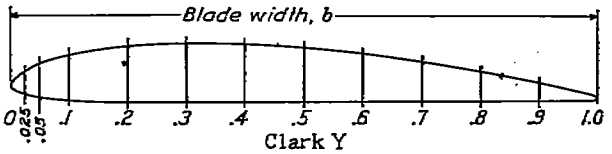

Clark Y

Station	Upper ordinate / Maximum ordinate	Lower ordinate / Maximum ordinate
0.025	0.55	0.13
.05	.67	.08
.1	.81	.04
.2	.96	.01
.3	1.00	0
.4	.99	0
.5	.93	0
.6	.83	0
.7	.69	0
.8	.52	0
.9	.34	0
L. E. radius		0.15
T. E. radius		.077

Clark Y

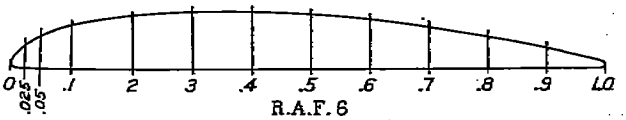

R.A.F. 6

Station	Ordinate / Maximum ordinate
0.025	0.41
.05	.59
.1	.79
.2	.95
.3	1.00
.4	.99
.5	.95
.6	.87
.7	.74
.8	.56
.9	.35
L. E. radius	0.10
T. E. radius	.077

R. A. F. 6

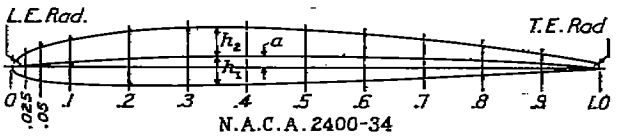

N.A.C.A. 2400-34

Station	a/b	$h_1/t=h_2/t$
0.025	0.00225	0.2160
.05	.00433	.2938
.1	.0085	.3845
.2	.0142	.4725
.3	.0135	.5000
.4	.0201	.4898
.5	.0198	.4538
.6	.0135	.4012
.7	.0161	.3363
.8	.0126	.2650
.9	.0085	.1638
L. E. radius		0.156
T. E. radius		.078

b, chord; t, thickness
N. A. C. A. 2400-34

FIGURE 9.—Basic propeller sections. Airfoil specifications taken from reference 6.

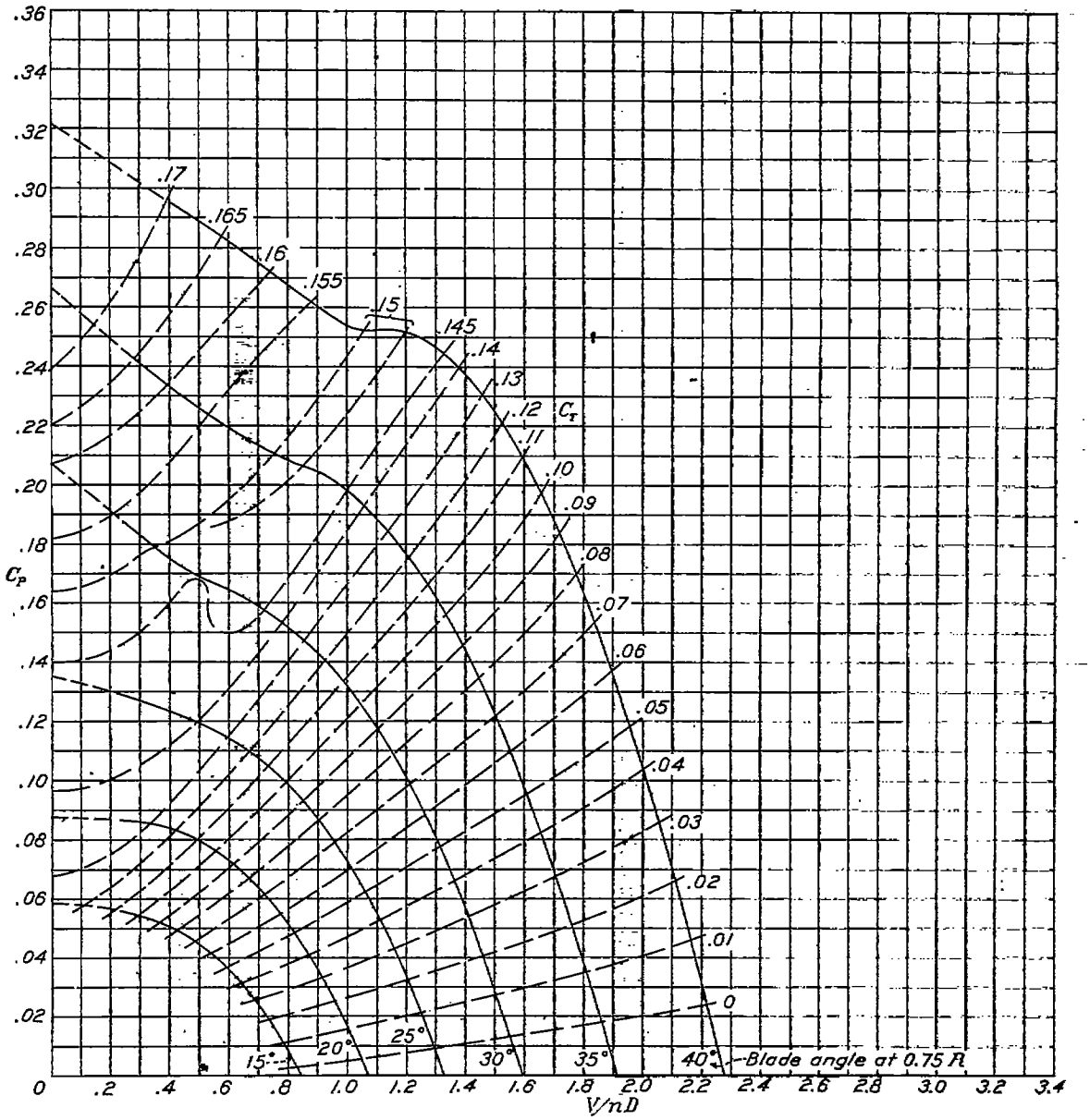

FIGURE 10.—Power-coefficient curves for propeller 5868-9, 3 blades, radial engine nacelle.

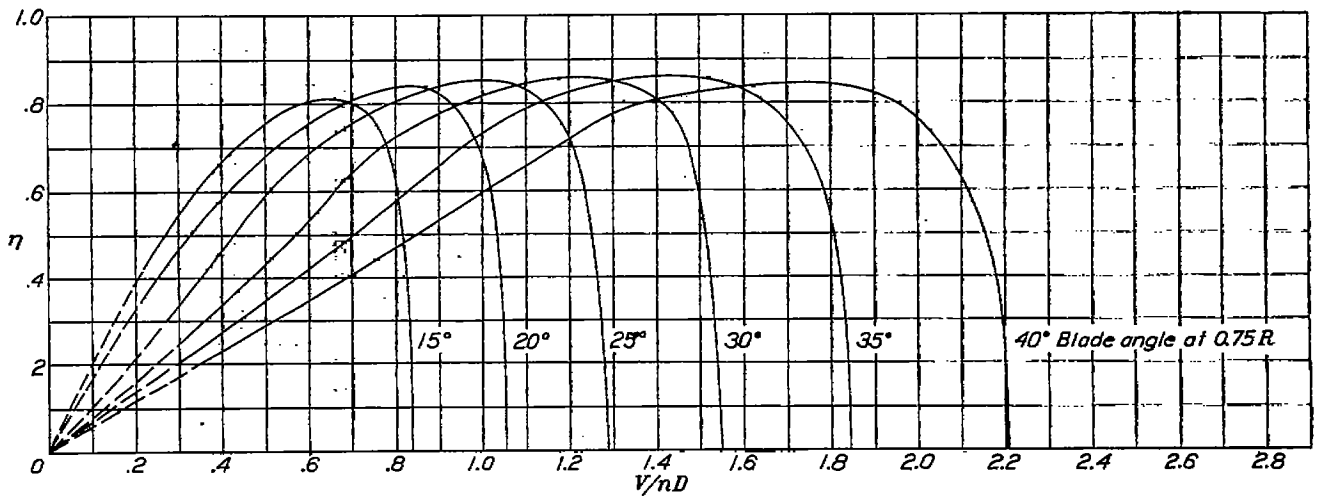

FIGURE 11.—Efficiency curves for propeller 5868-9, 3 blades, radial engine nacelle.

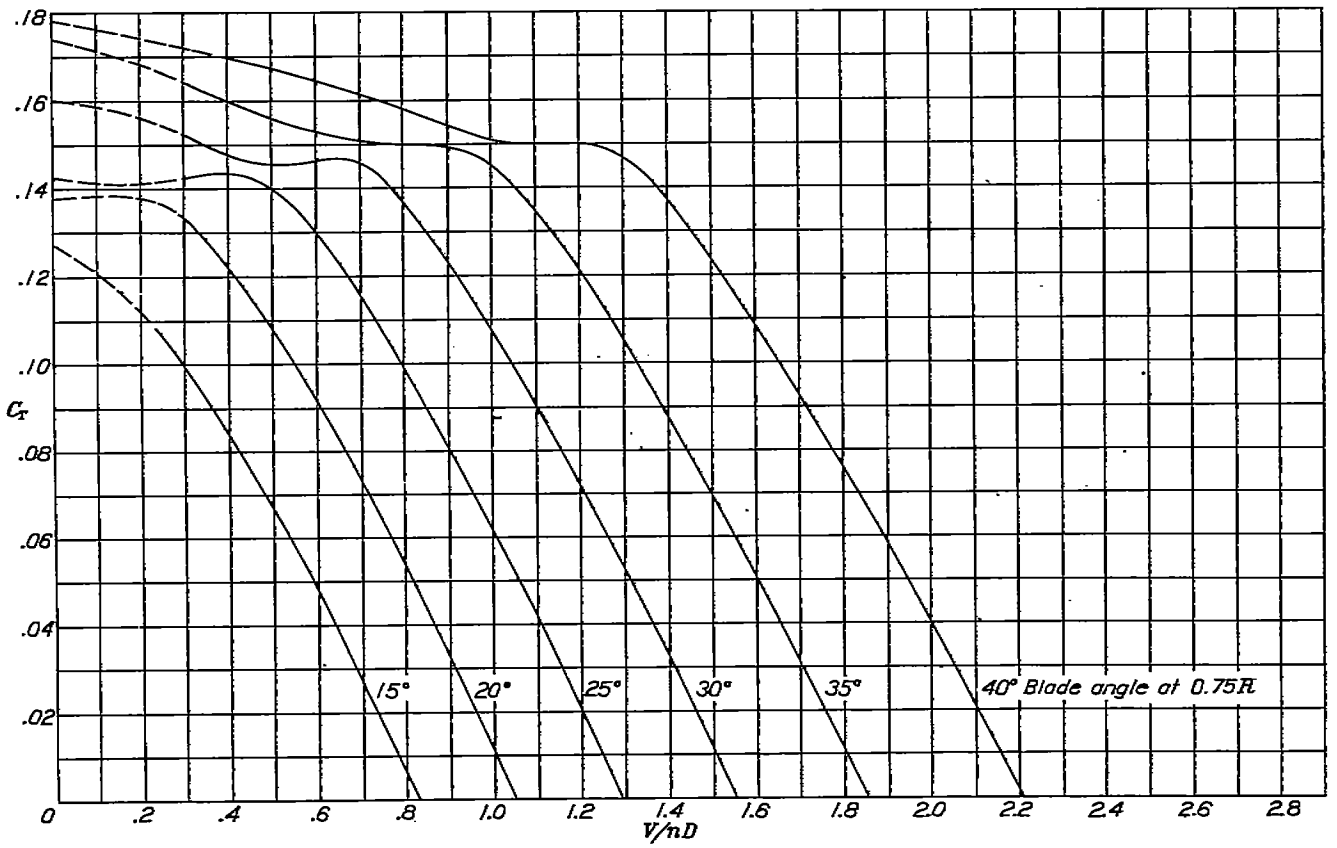

FIGURE 12.—Thrust-coefficient curves for propeller 5868-9, 3 blades, radial engine nacelle.

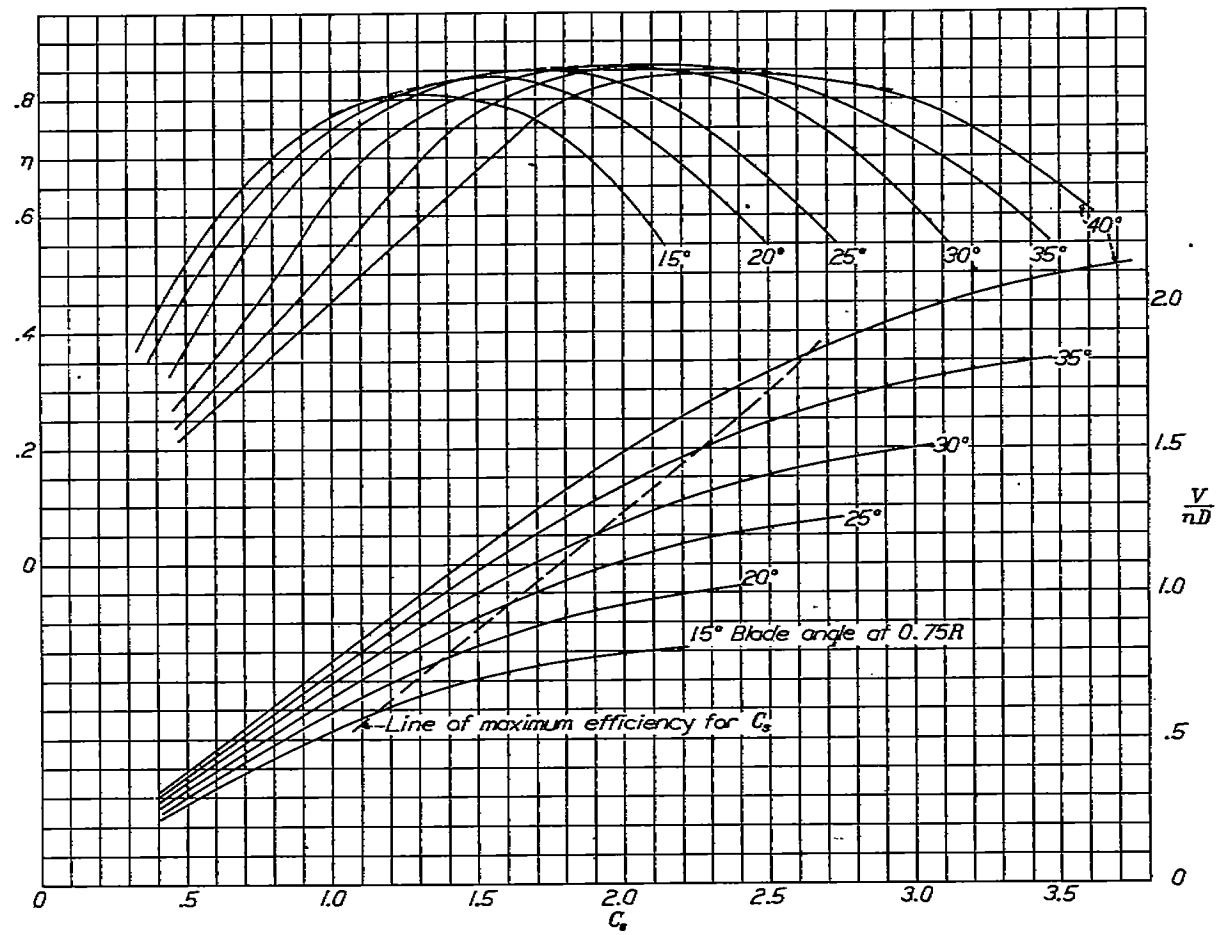

FIGURE 13.—Design chart for propeller 5868-9, 3 blades, radial engine nacelle.

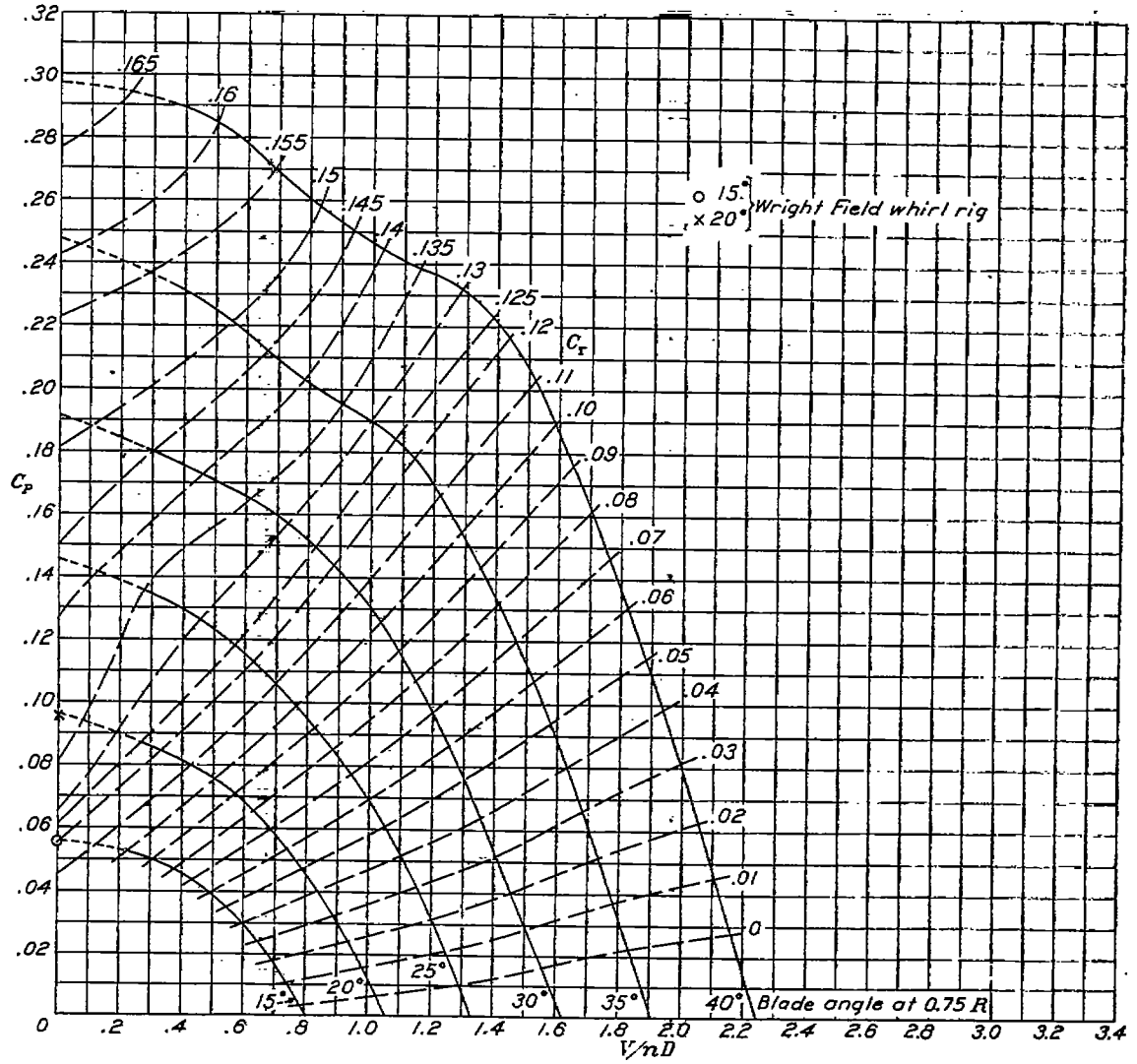

FIGURE 14.—Power-coefficient curves for propeller 6101, 3 blades, radial engine nacelle.

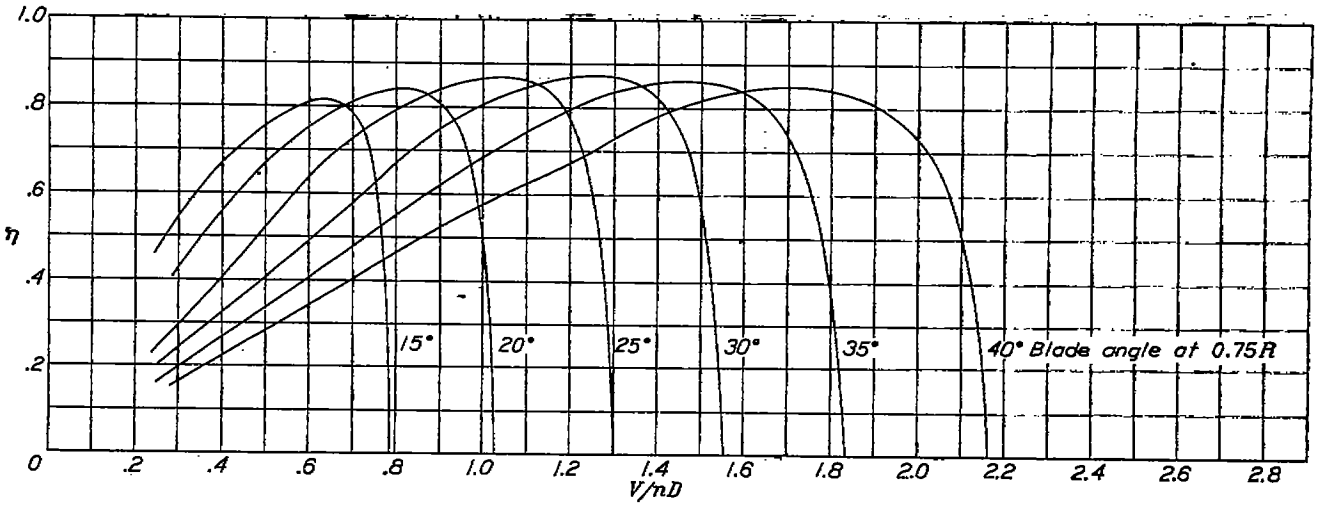

FIGURE 15.—Efficiency curves for propeller 6101, 3 blades, radial engine nacelle.

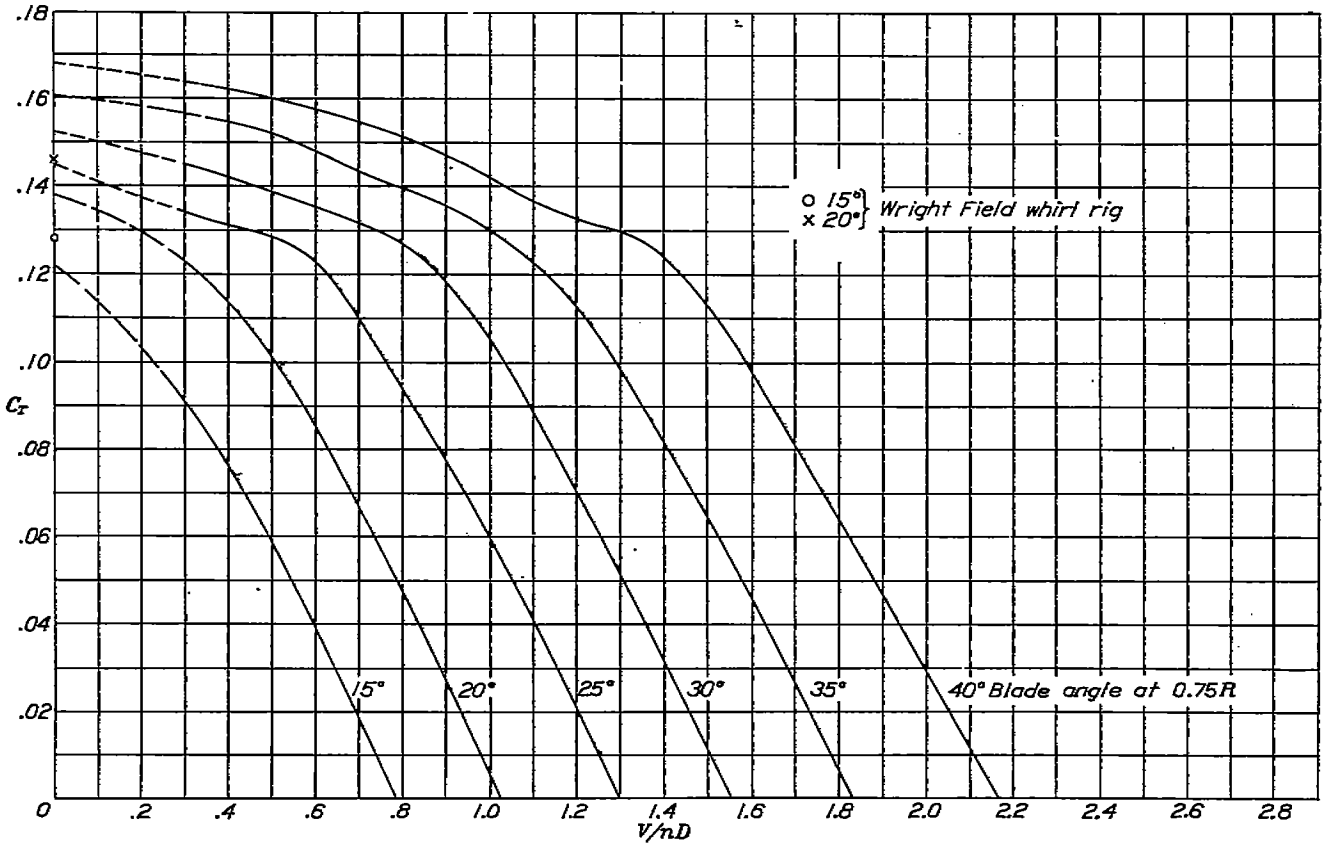

FIGURE 16.—Thrust-coefficient curves for propeller 6101, 3 blades, radial engine nacelle.

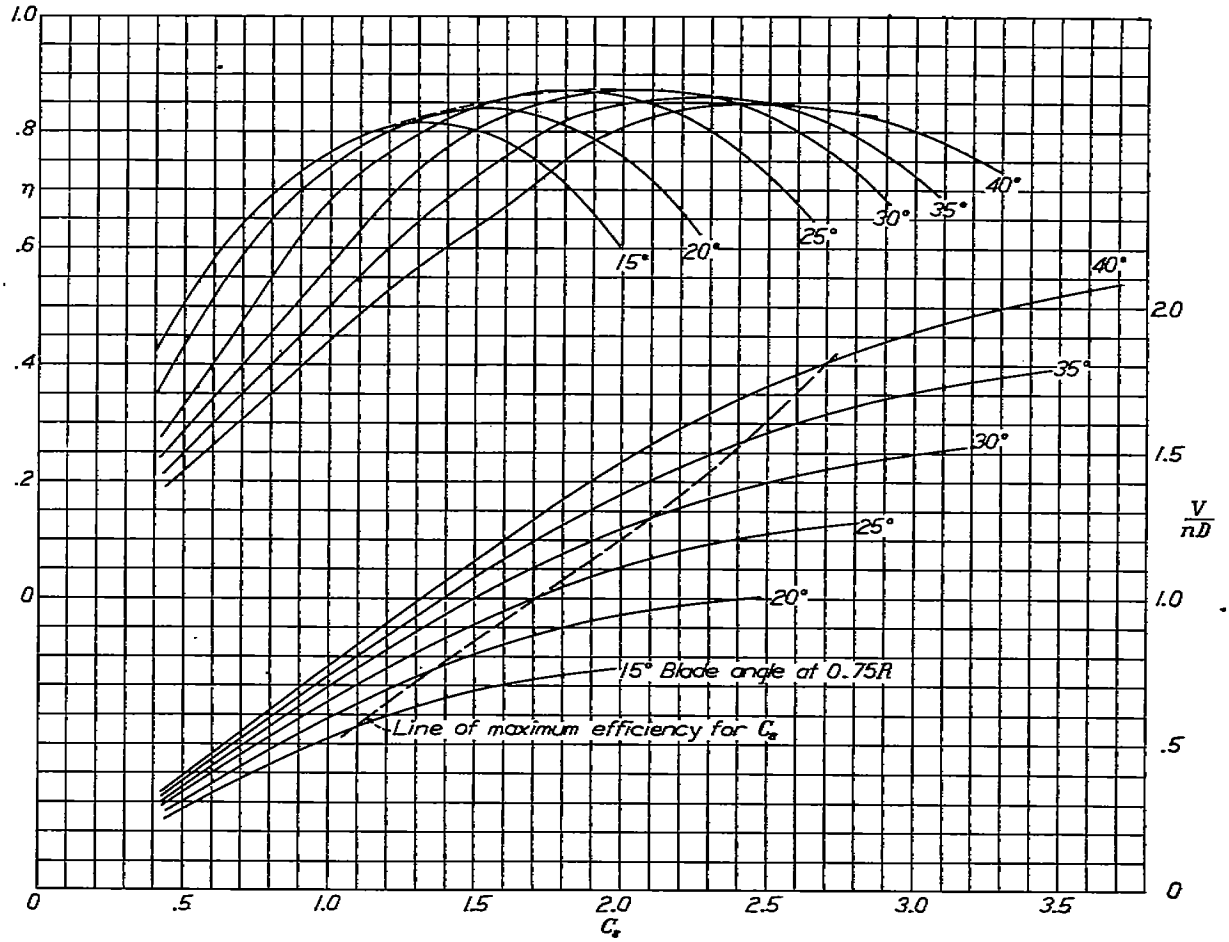

FIGURE 17.—Design chart for propeller 6101, 3 blades, radial engine nacelle.

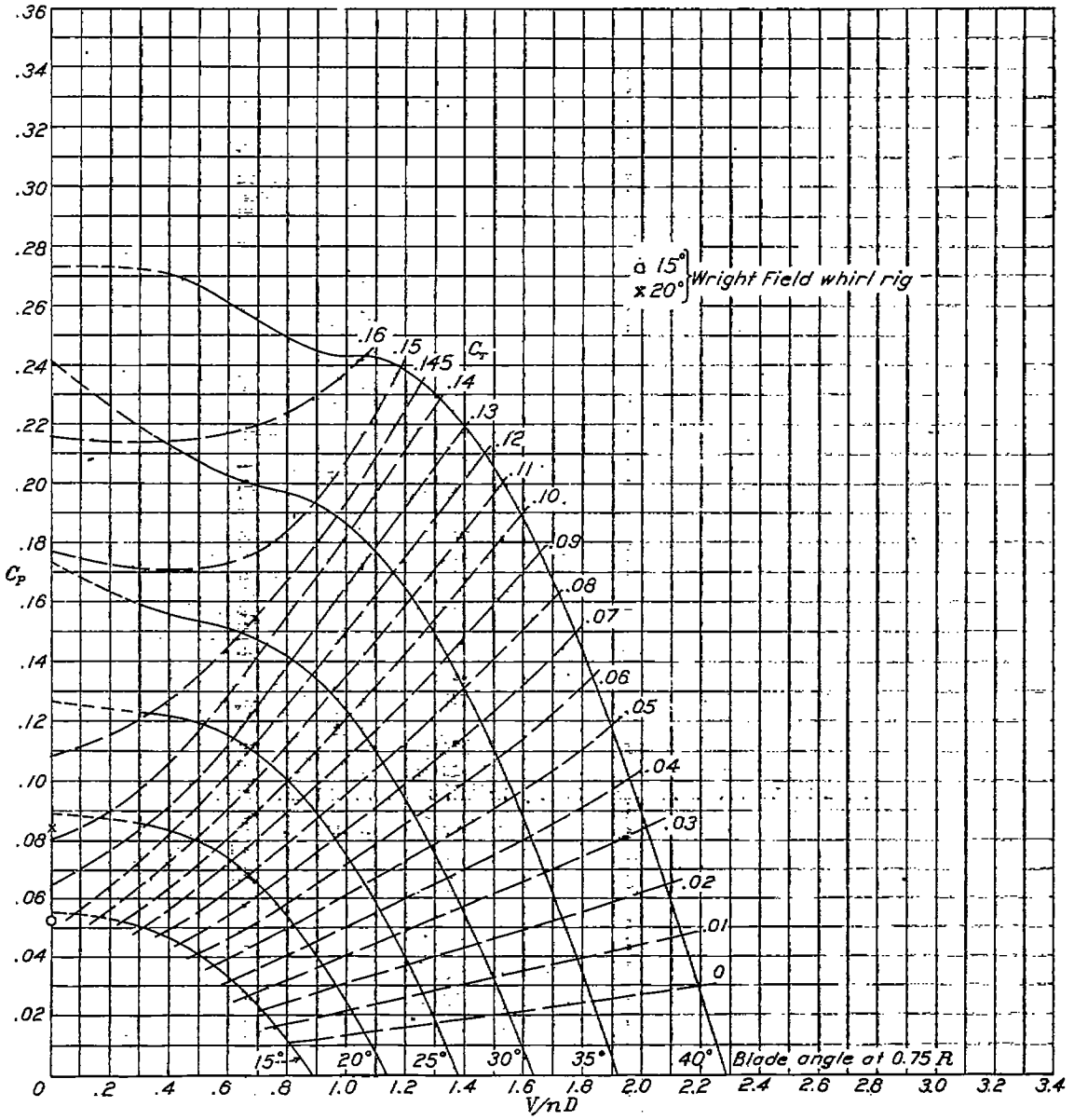

FIGURE 18.—Power-coefficient curves for propeller 6129, 3 blades, radial engine nacelle.

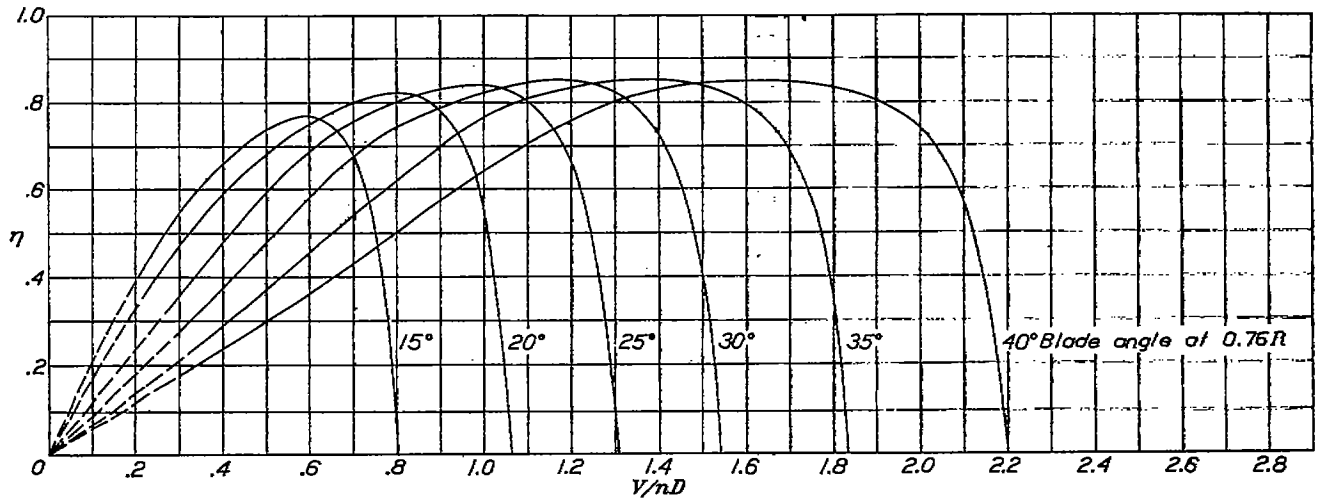

FIGURE 19.—Efficiency curves for propeller 6129, 3 blades, radial engine nacelle.

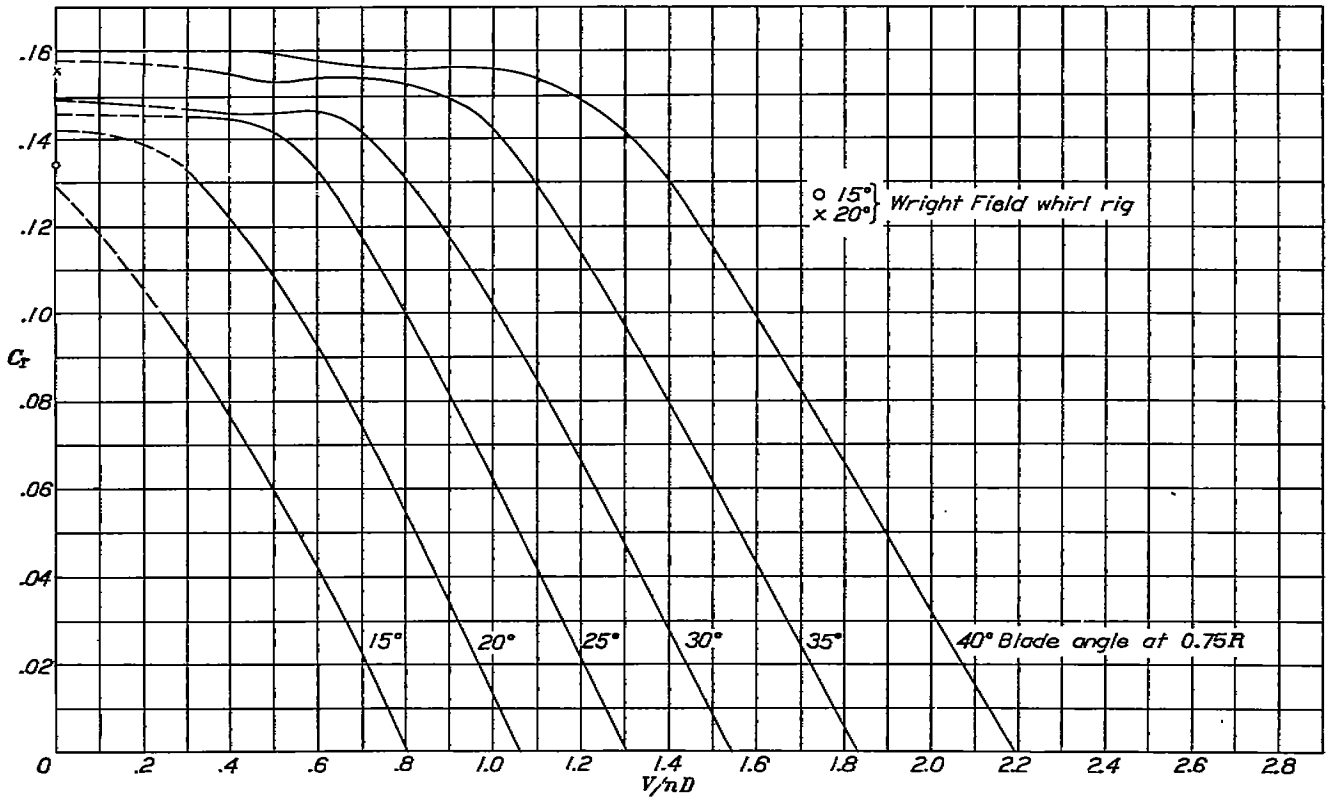

FIGURE 20.—Thrust-coefficient curves for propeller 6129, 3 blades, radial engine nacelle.

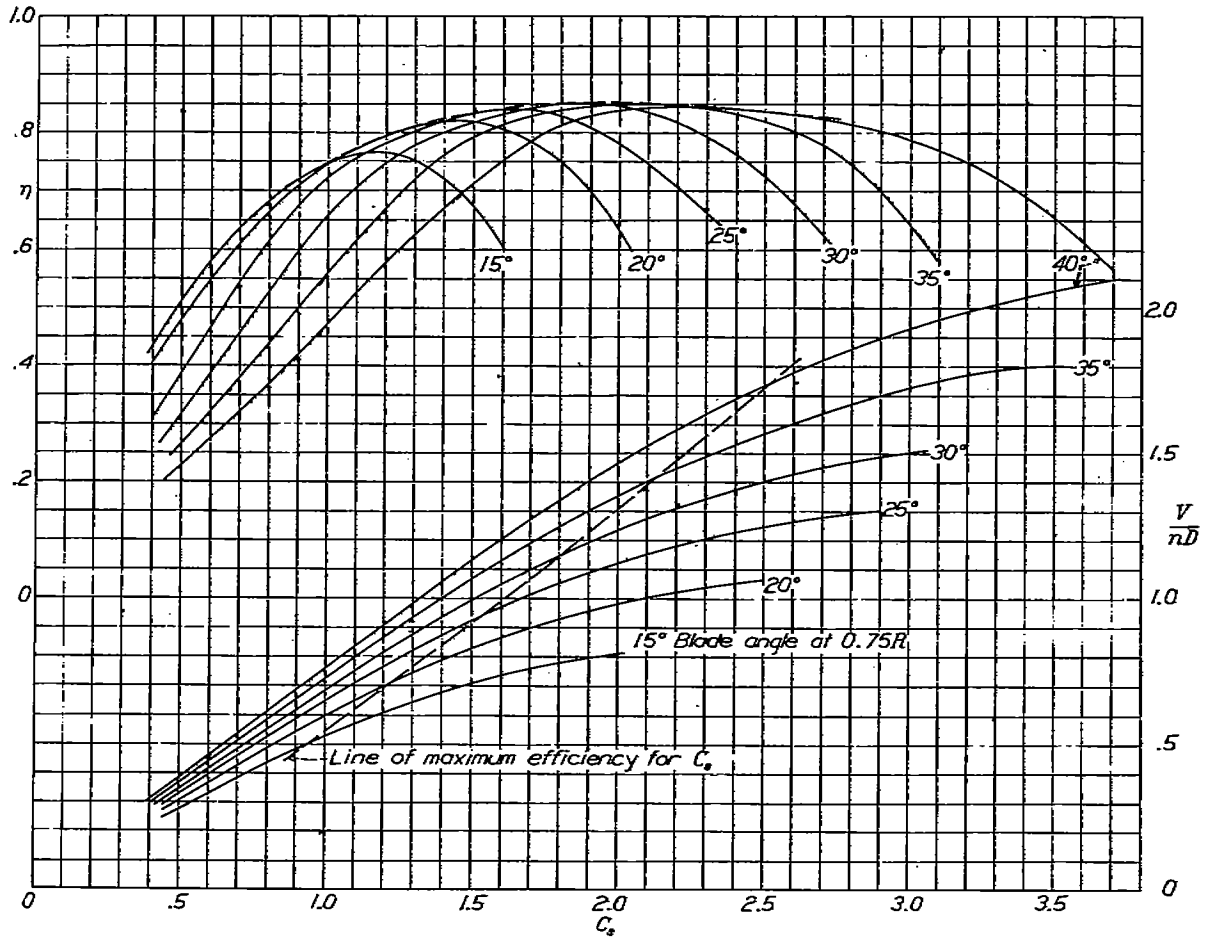

FIGURE 21.—Design chart for propeller 6129, 3 blades, radial engine nacelle.

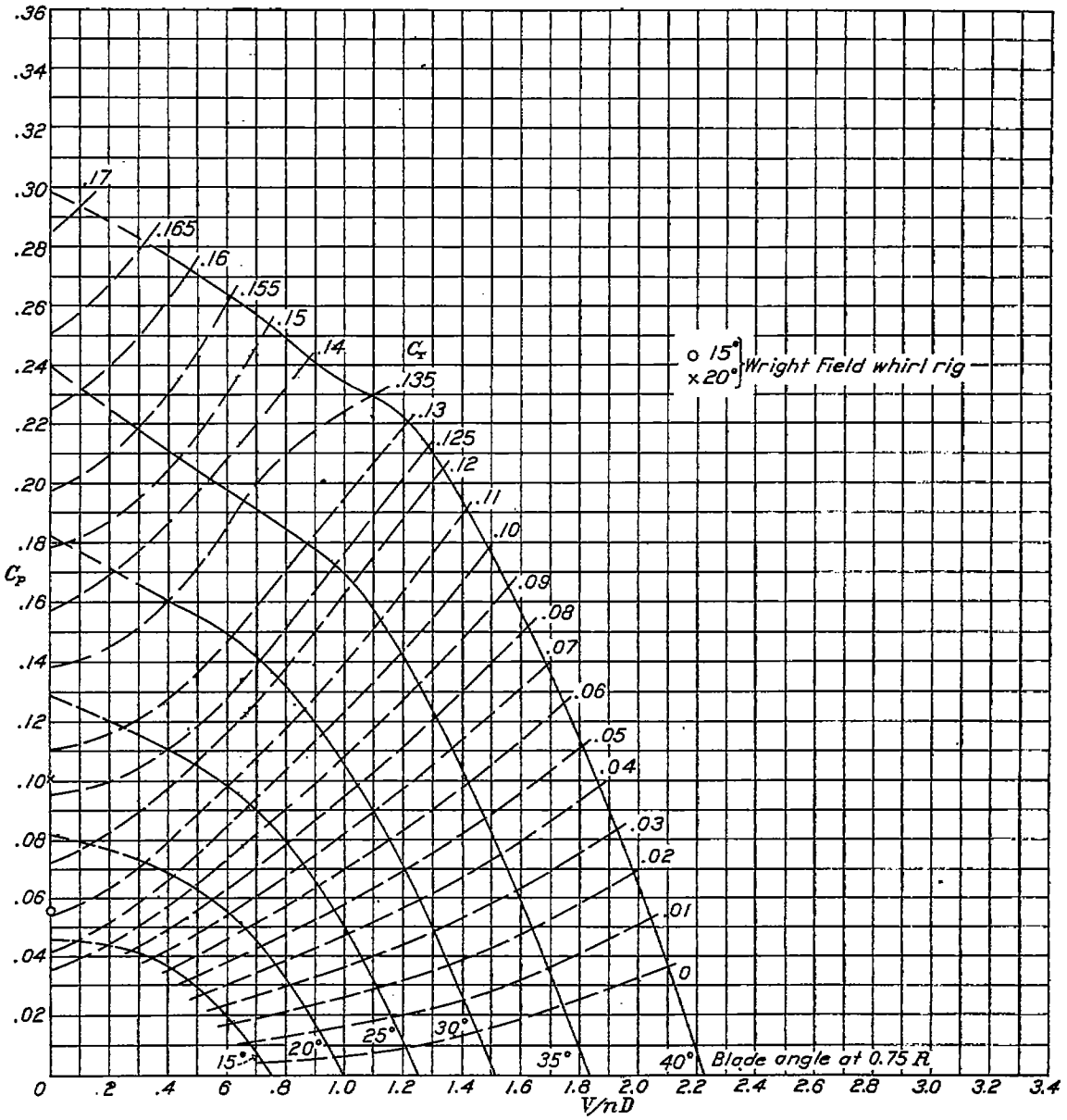

FIGURE 22.—Power-coefficient curves for propeller 6131, 3 blades, radial engine nacelle.

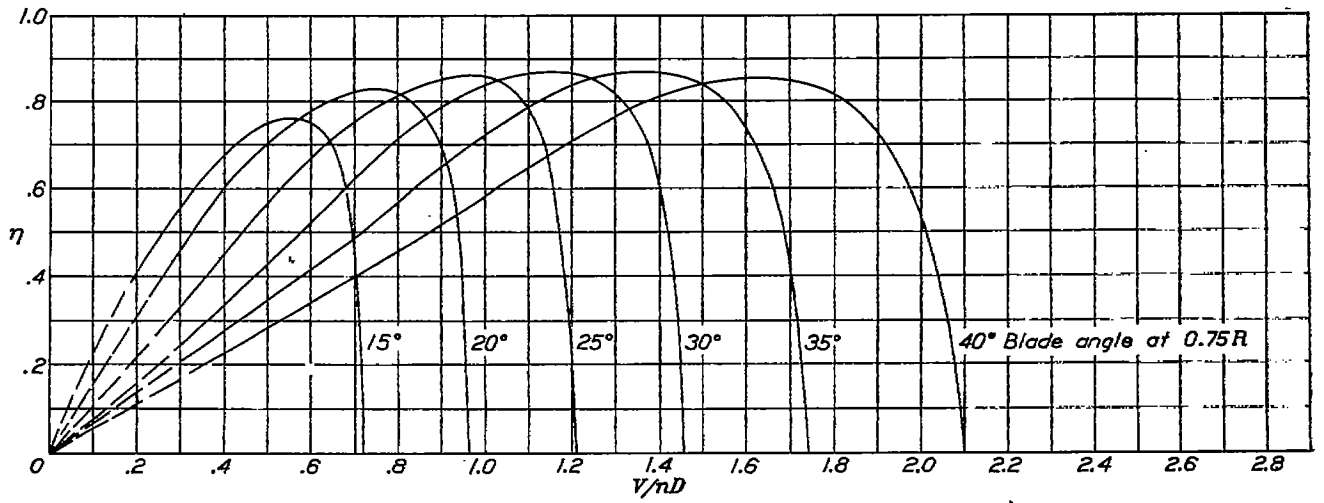

FIGURE 23.—Efficiency curves for propeller 6131, 3 blades, radial engine nacelle.

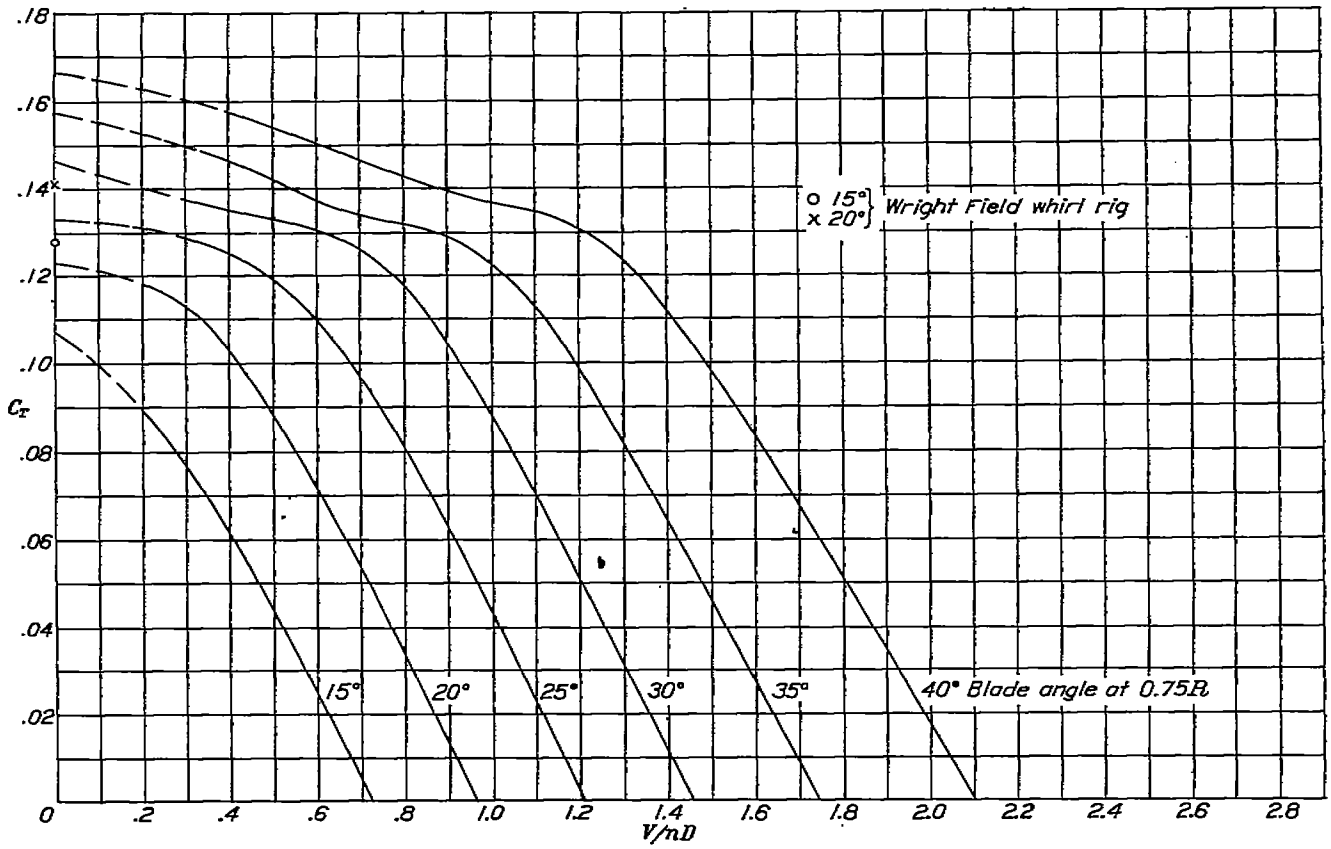

FIGURE 24.—Thrust-coefficient curves for propeller 6131, 3 blades, radial engine nacelle

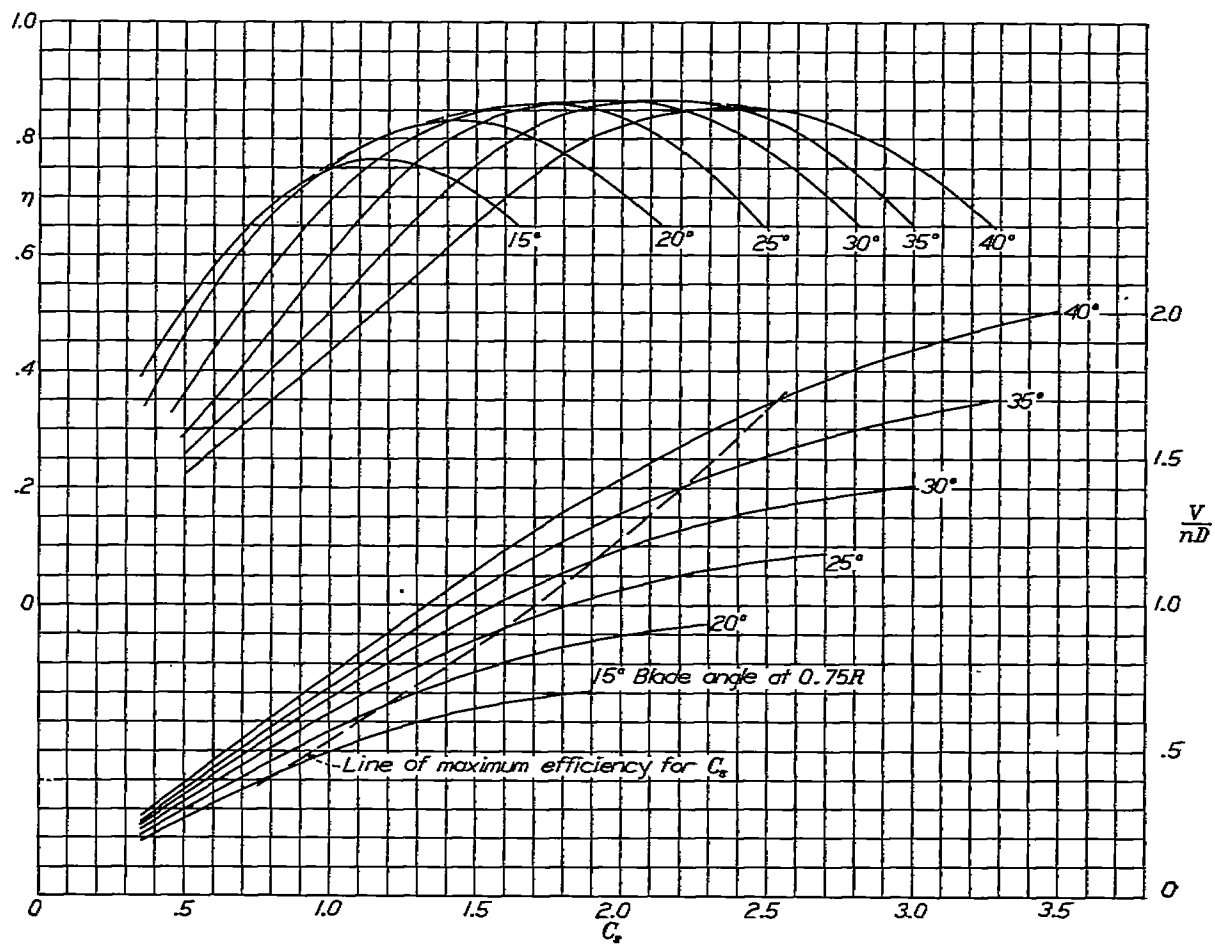

FIGURE 25.—Design chart for propeller 6131, 3 blades, radial engine nacelle.

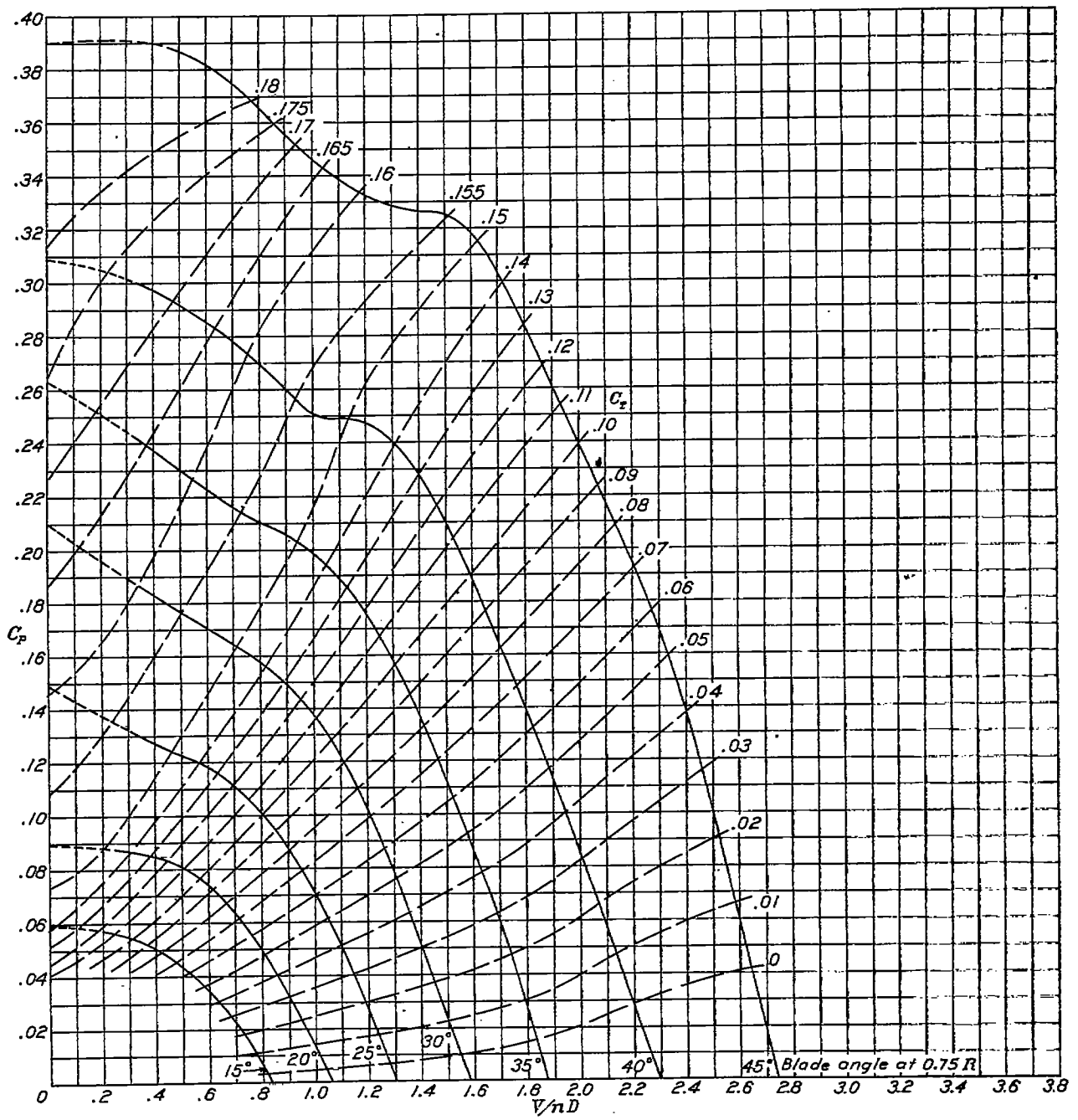

FIGURE 26.—Power-coefficient curves for propeller 5868-9, 3 blades, liquid-cooled engine nacelle.

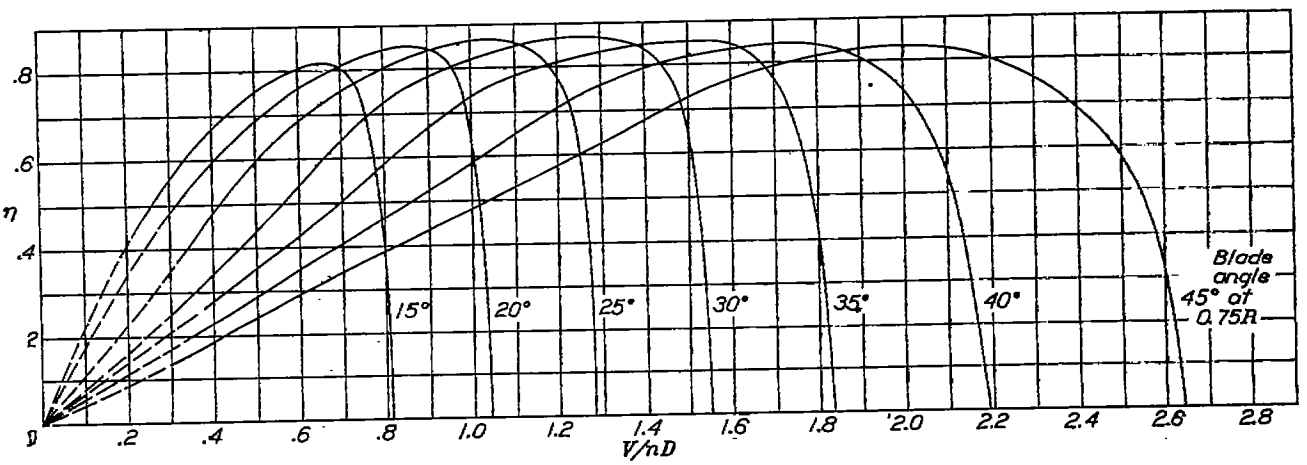

FIGURE 27.—Efficiency curves for propeller 5868-9, 3 blades, liquid-cooled engine nacelle.

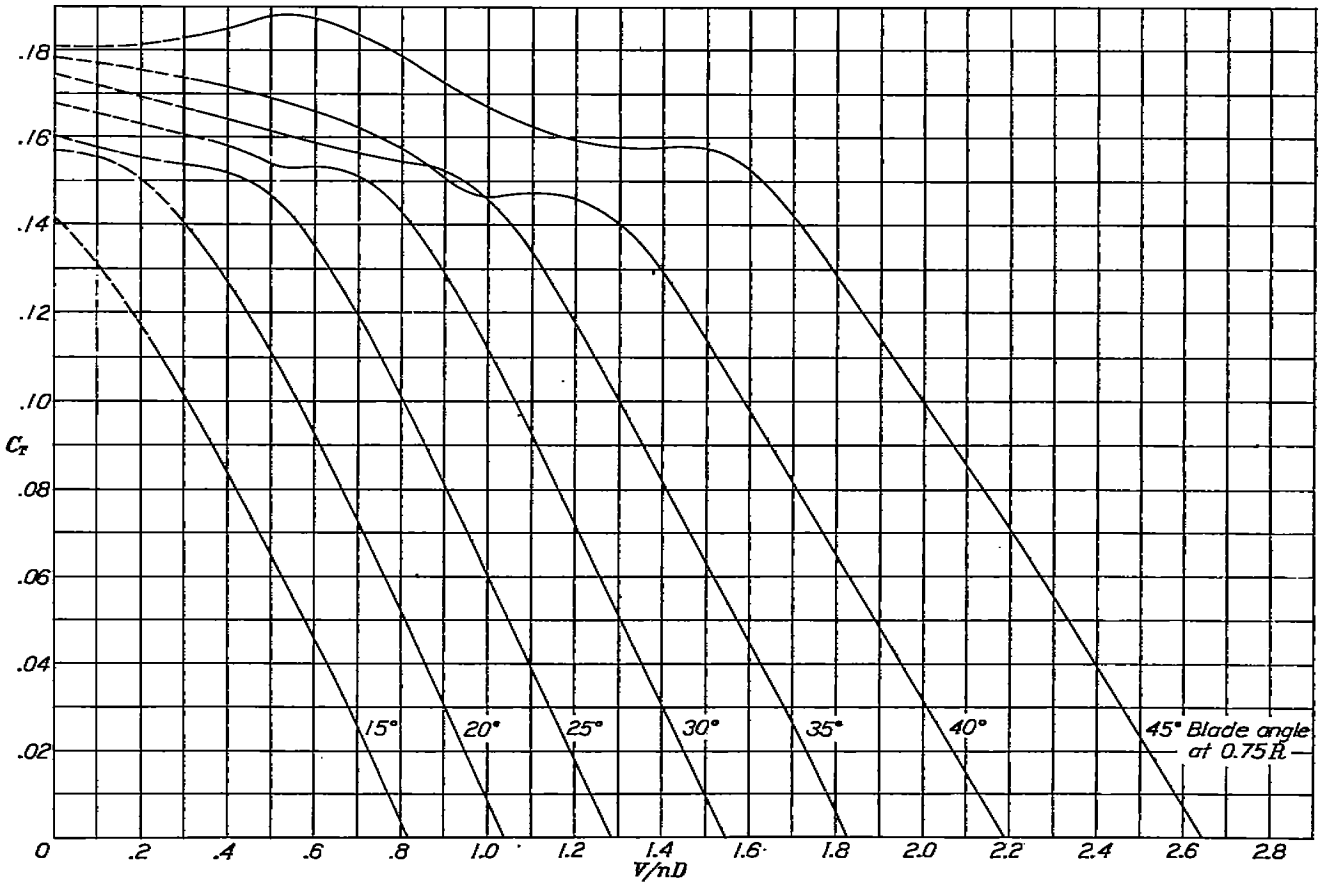

FIGURE 28.—Thrust-coefficient curves for propeller 5868-9, 3 blades, liquid-cooled engine nacelle.

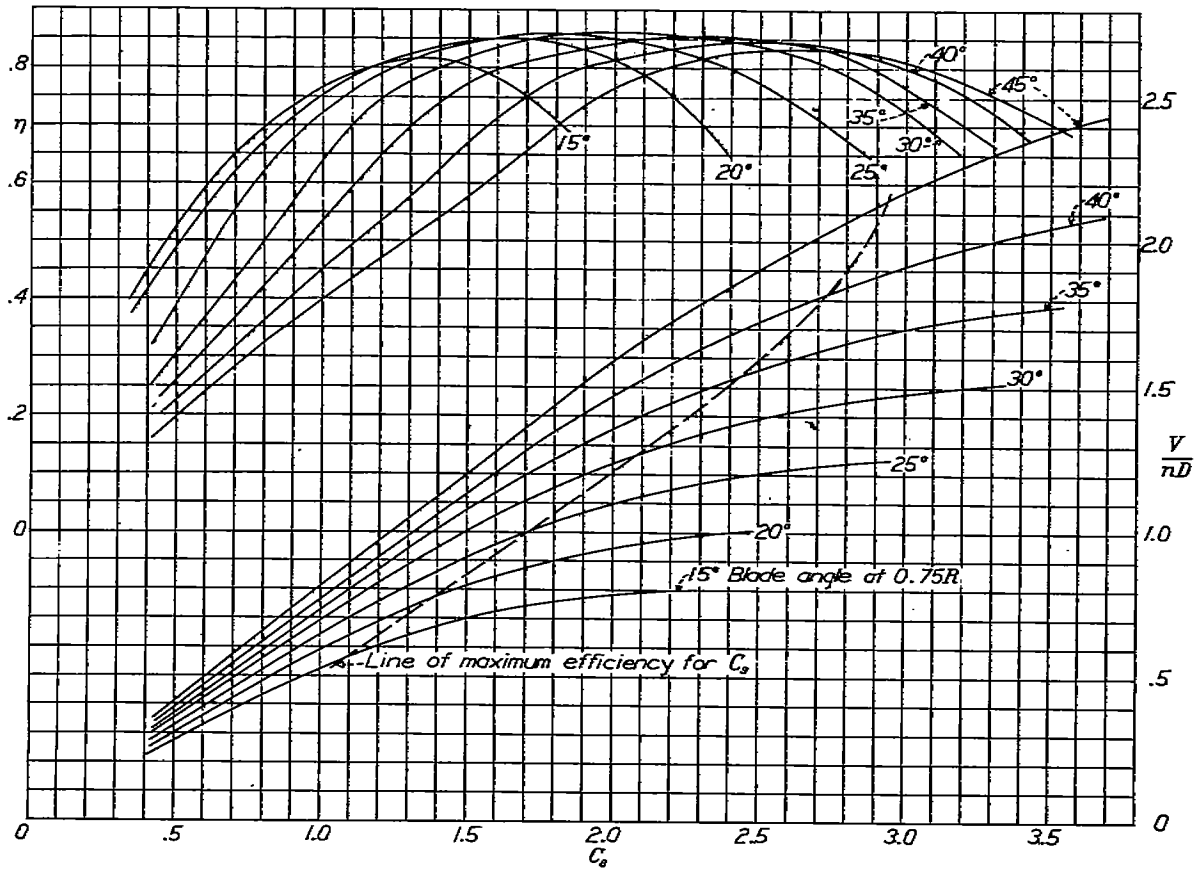

FIGURE 29.—Design chart for propeller 5868-9, 3 blades, liquid-cooled engine nacelle.

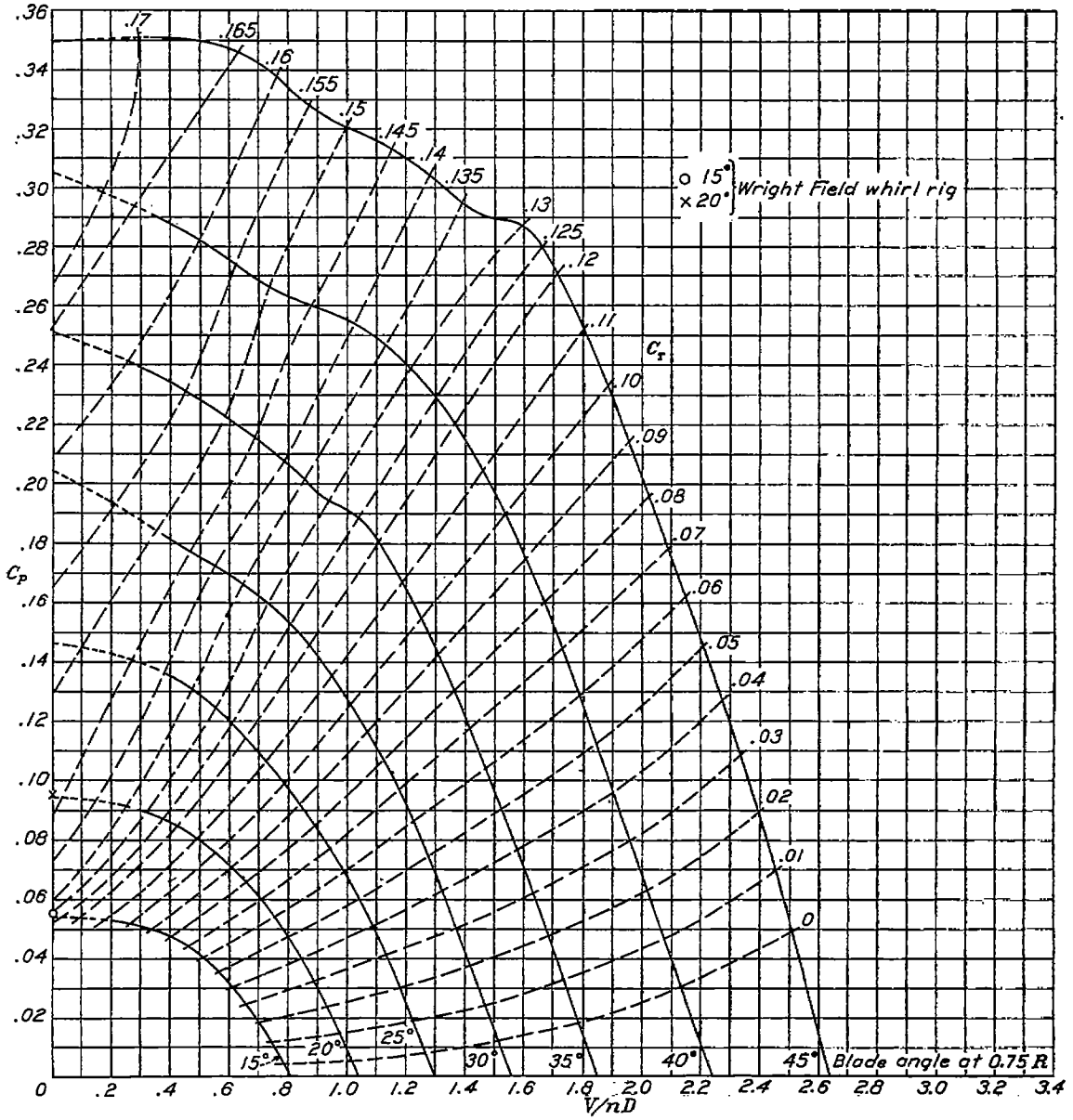

FIGURE 30.—Power-coefficient curves for propeller 6101, 3 blades, liquid-cooled engine nacelle.

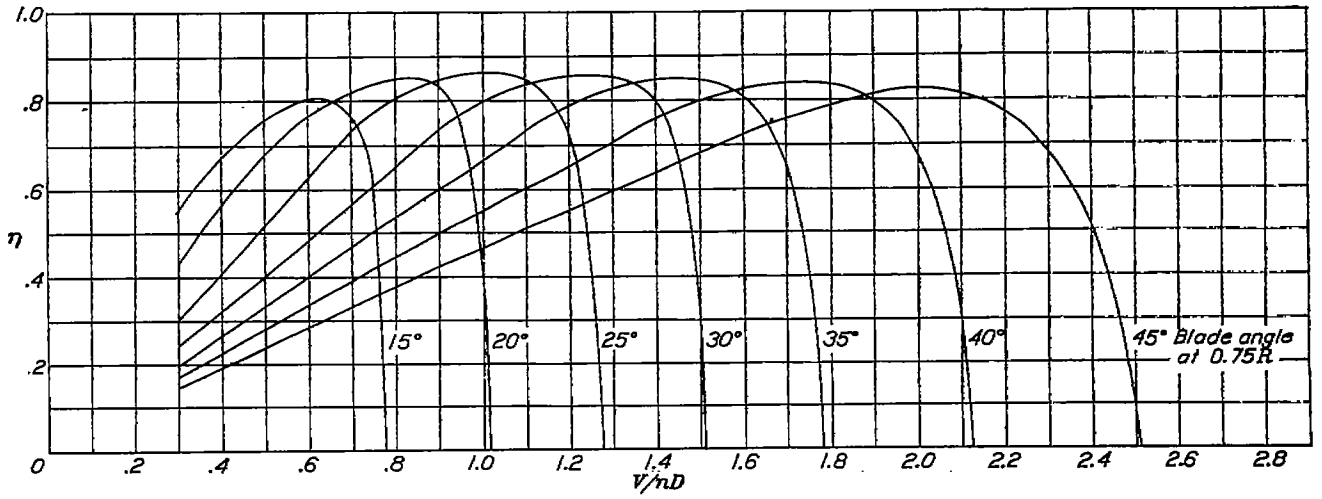

FIGURE 31.—Efficiency curves for propeller 6101, 3 blades, liquid-cooled engine nacelle.

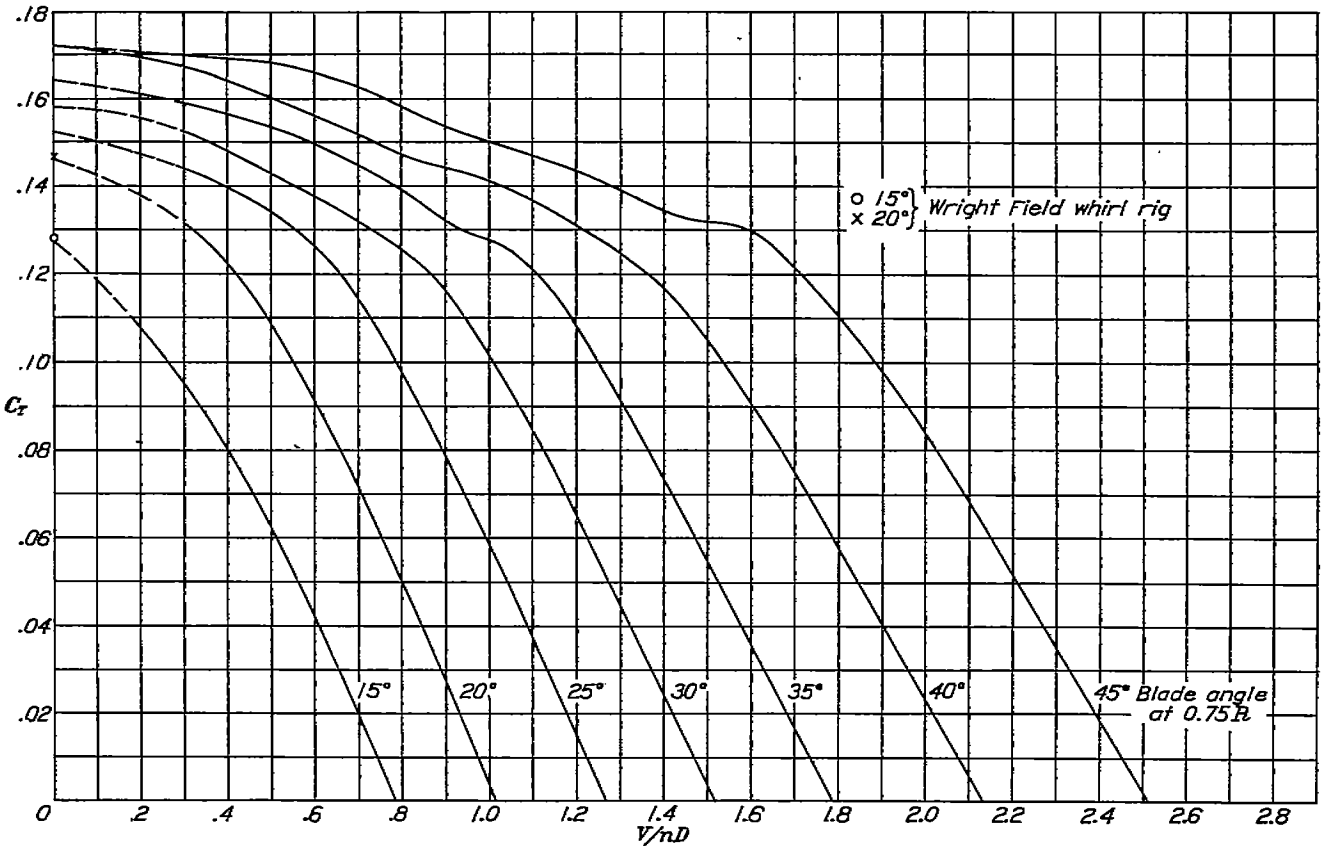

FIGURE 32.—Thrust-coefficient curves for propeller 6101, 3 blades, liquid-cooled engine nacelle.

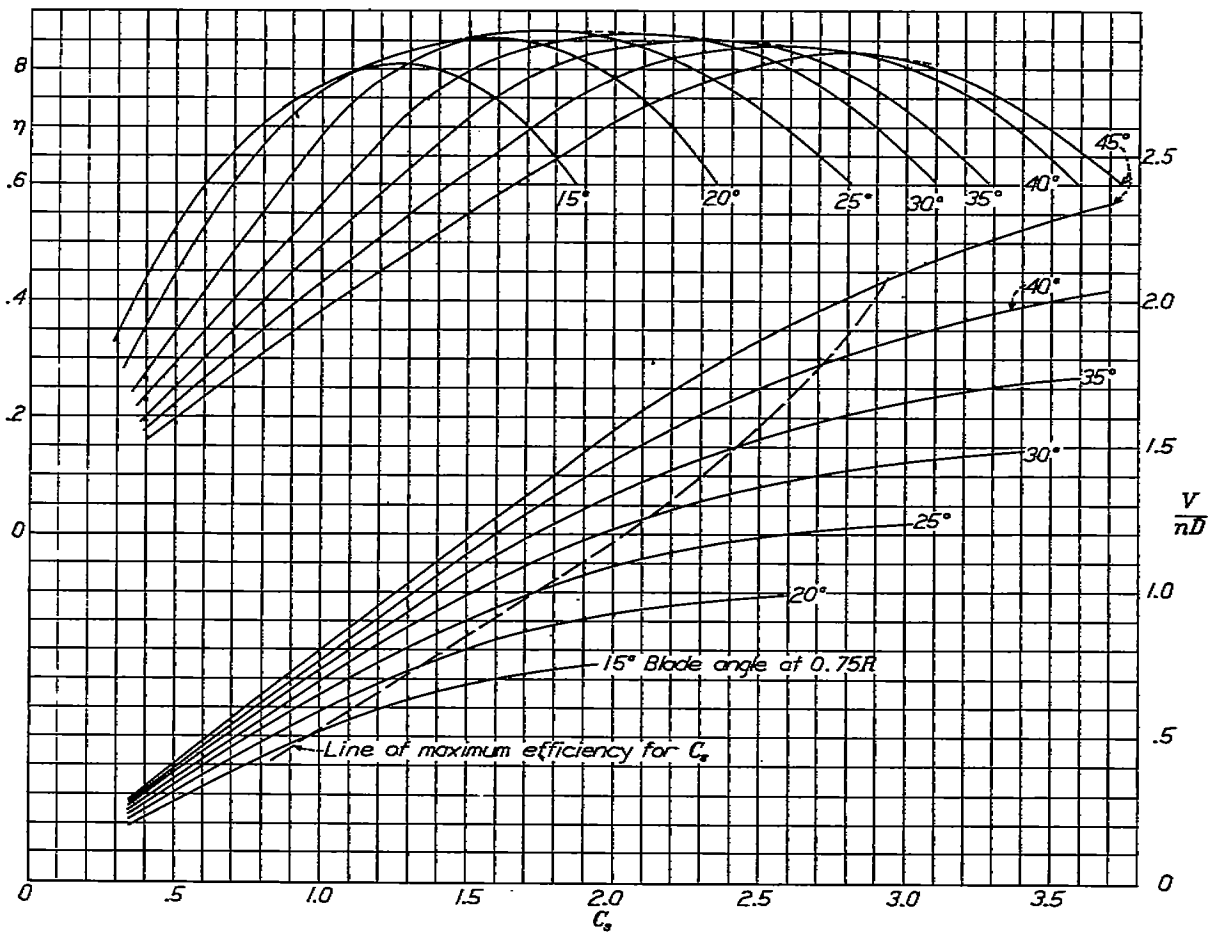

FIGURE 33.—Design chart for propeller 6101, 3 blades, liquid-cooled engine nacelle.

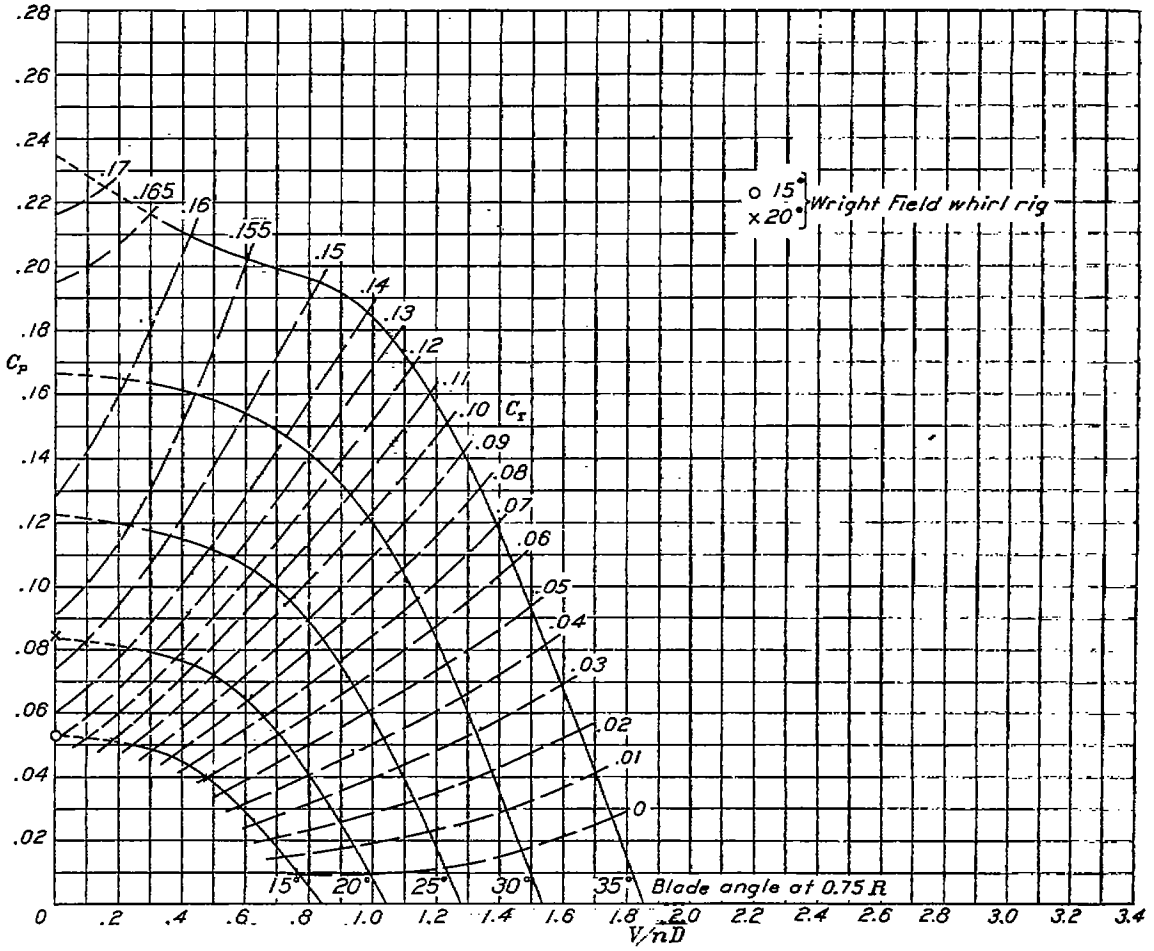

FIGURE 34.—Power-coefficient curves for propeller 6129, 3 blades, liquid-cooled engine nacelle.

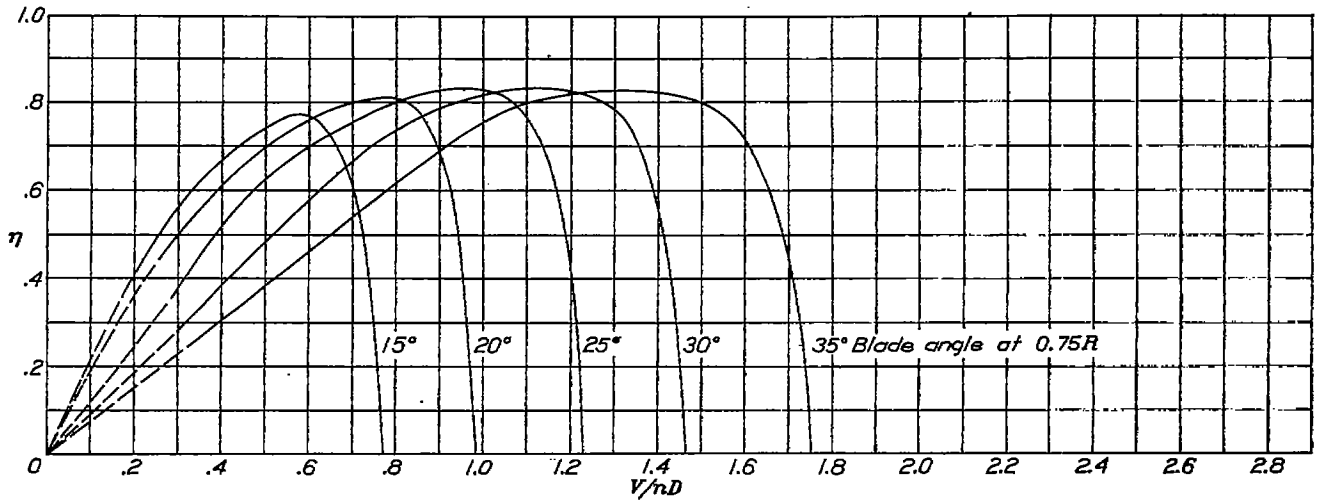

FIGURE 35.—Efficiency curves for propeller 6129, 3 blades, liquid-cooled engine nacelle.

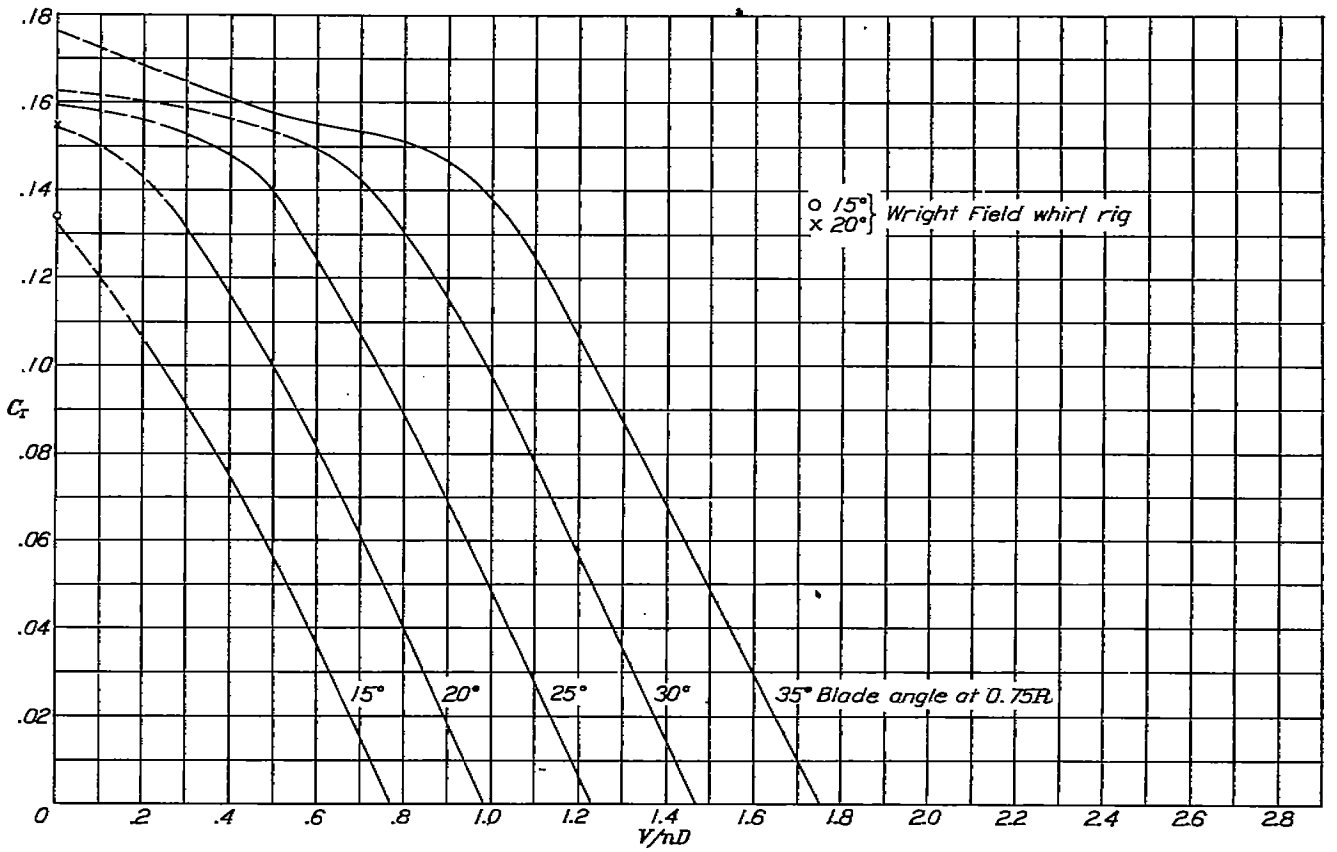

FIGURE 36.—Thrust-coefficient curves for propeller 6129, 3 blades, liquid-cooled engine nacelle.

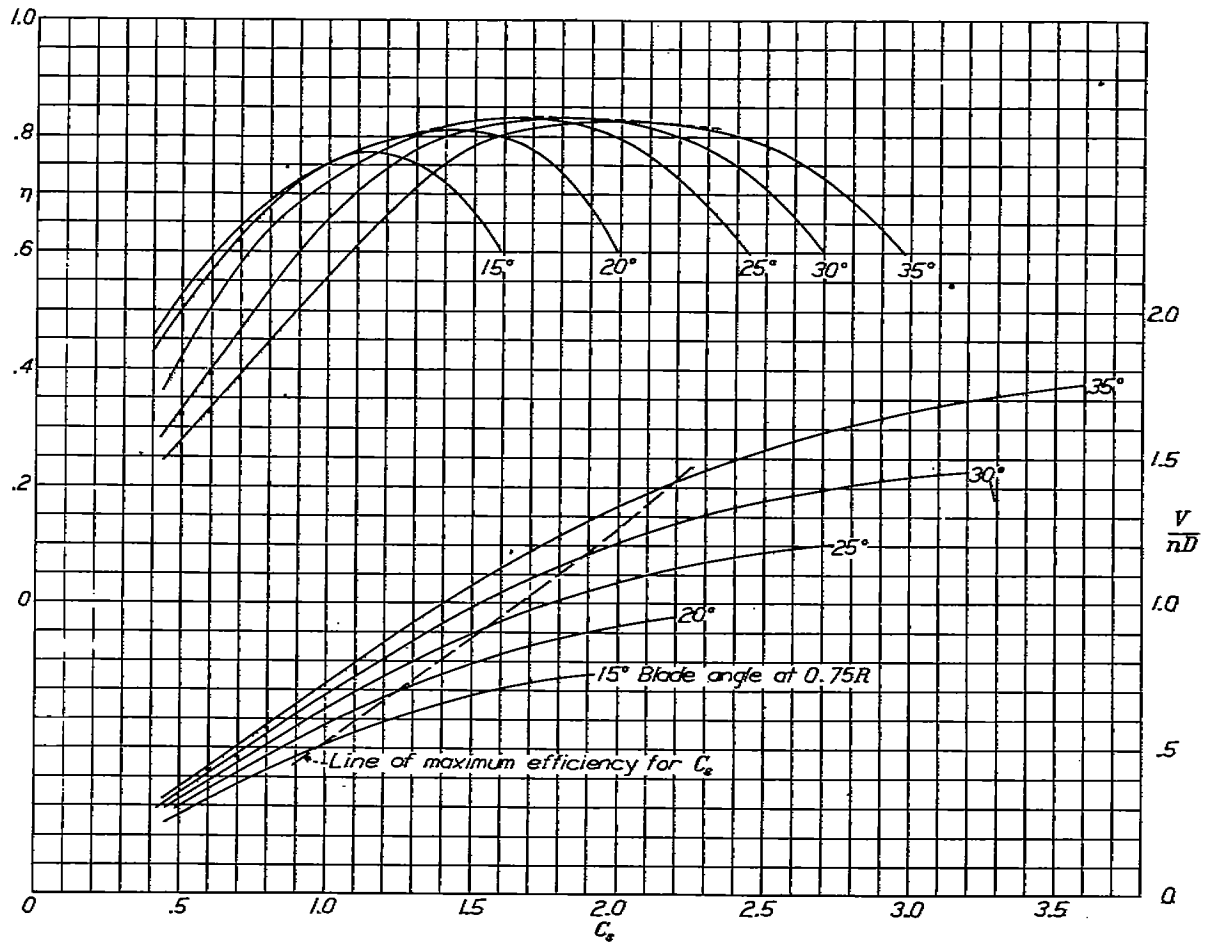

FIGURE 37.—Design chart for propeller 6129, 3 blades, liquid-cooled engine nacelle.

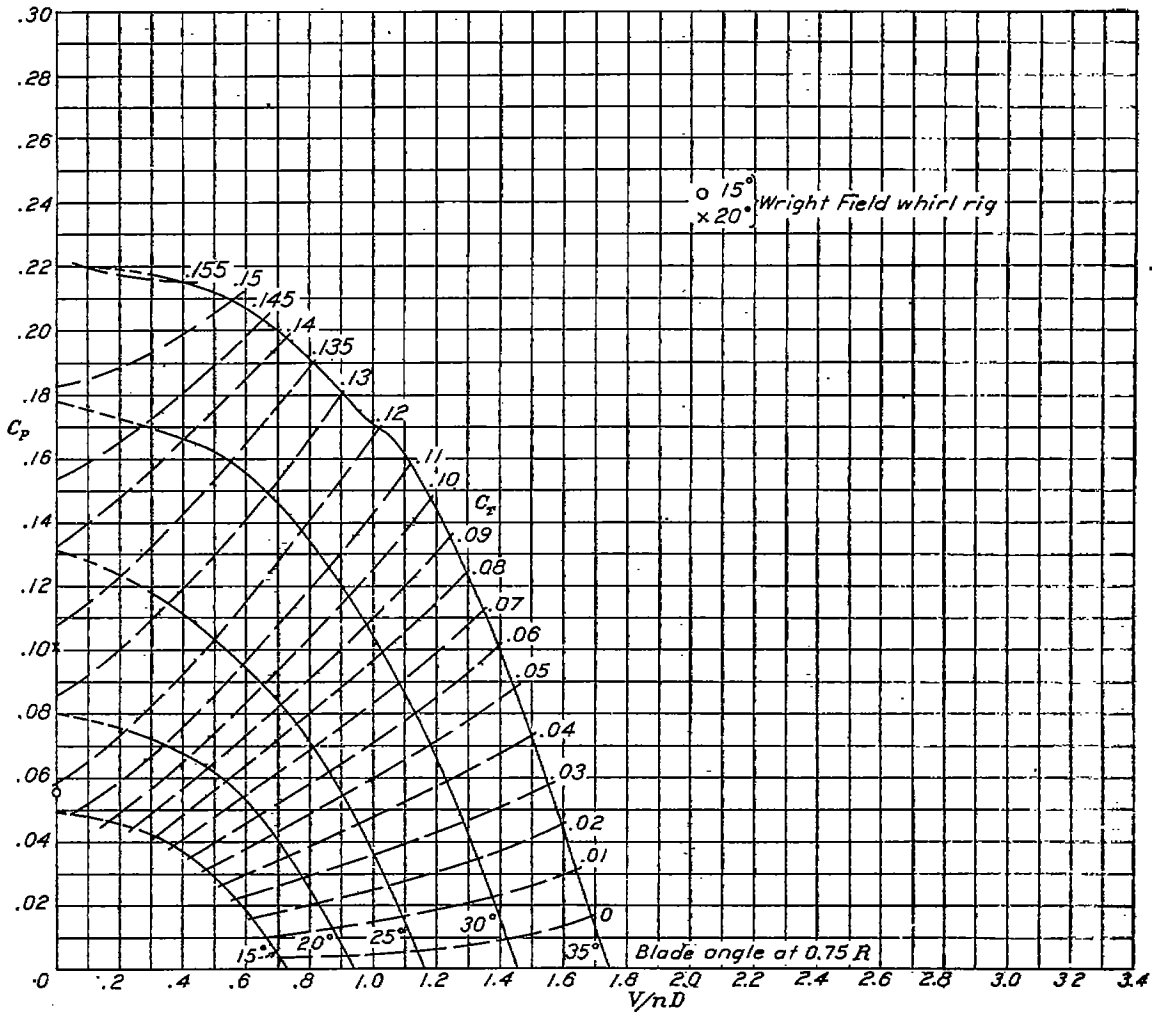

FIGURE 38.—Power-coefficient curves for propeller 6131, 3 blades, liquid-cooled engine nacelle.

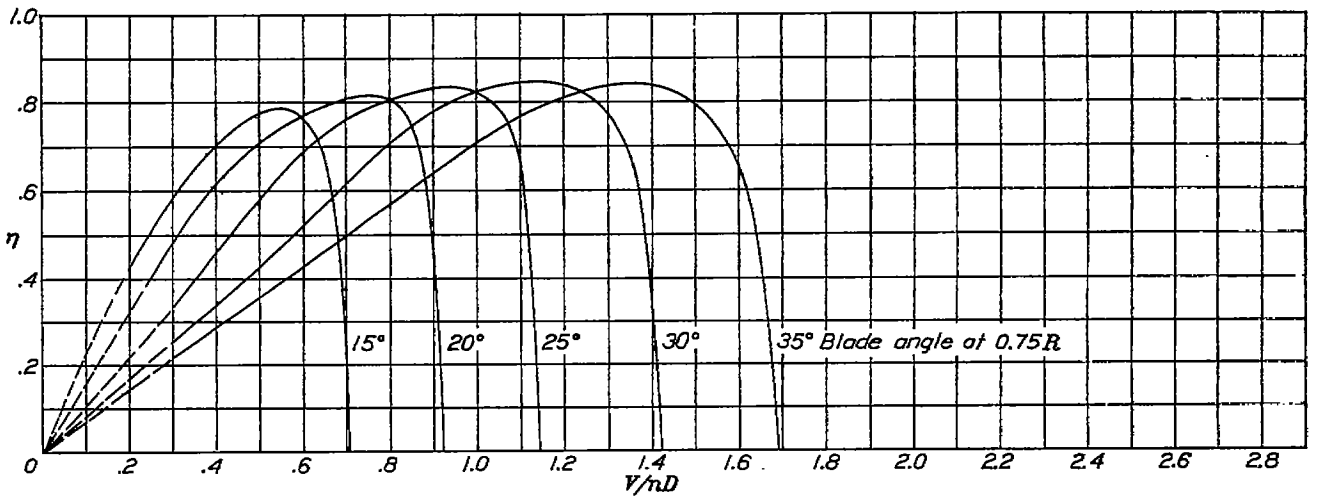

FIGURE 39.—Efficiency curves for propeller 6131, 3 blades, liquid-cooled engine nacelle.

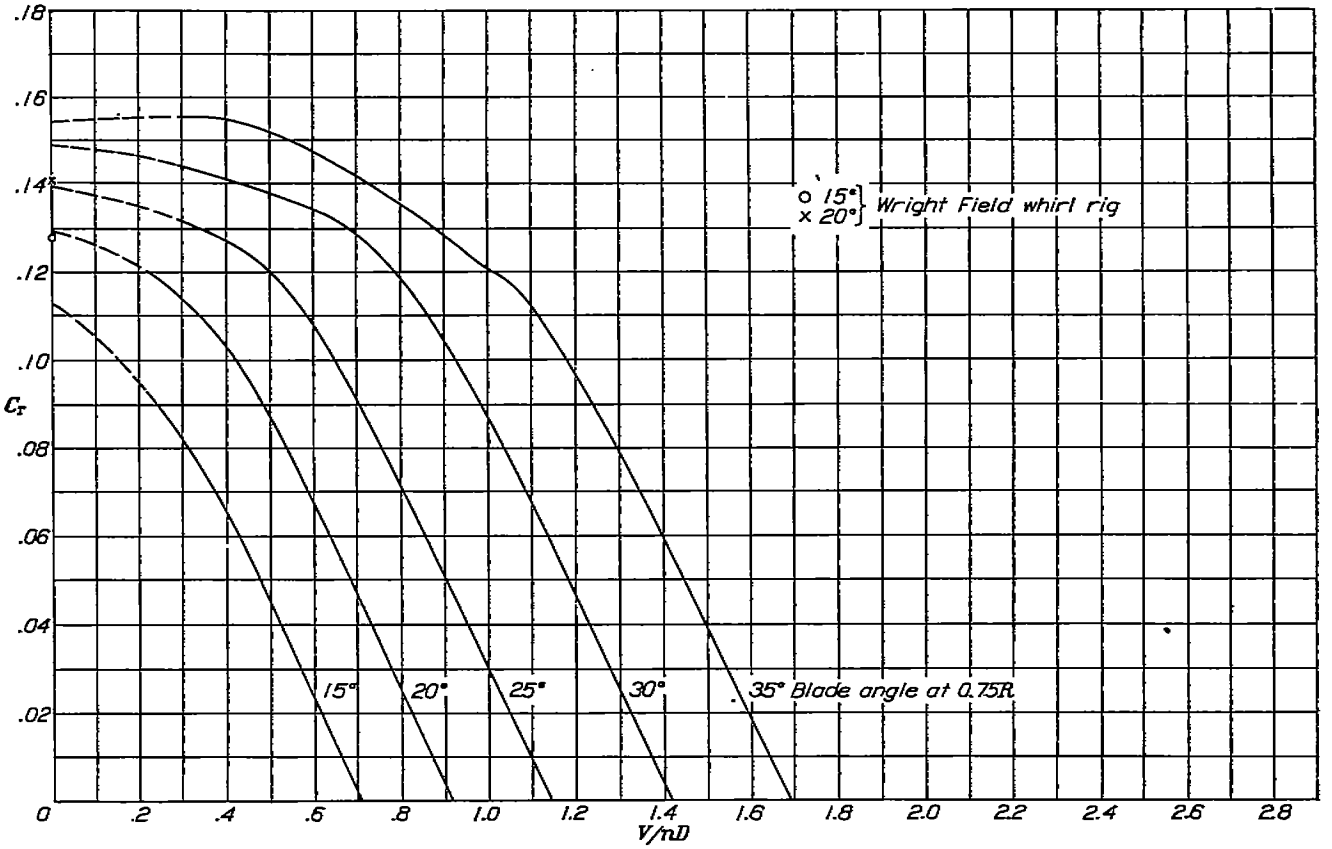

FIGURE 40.—Thrust-coefficient curves for propeller 6131, 3 blades, liquid-cooled engine nacelle.

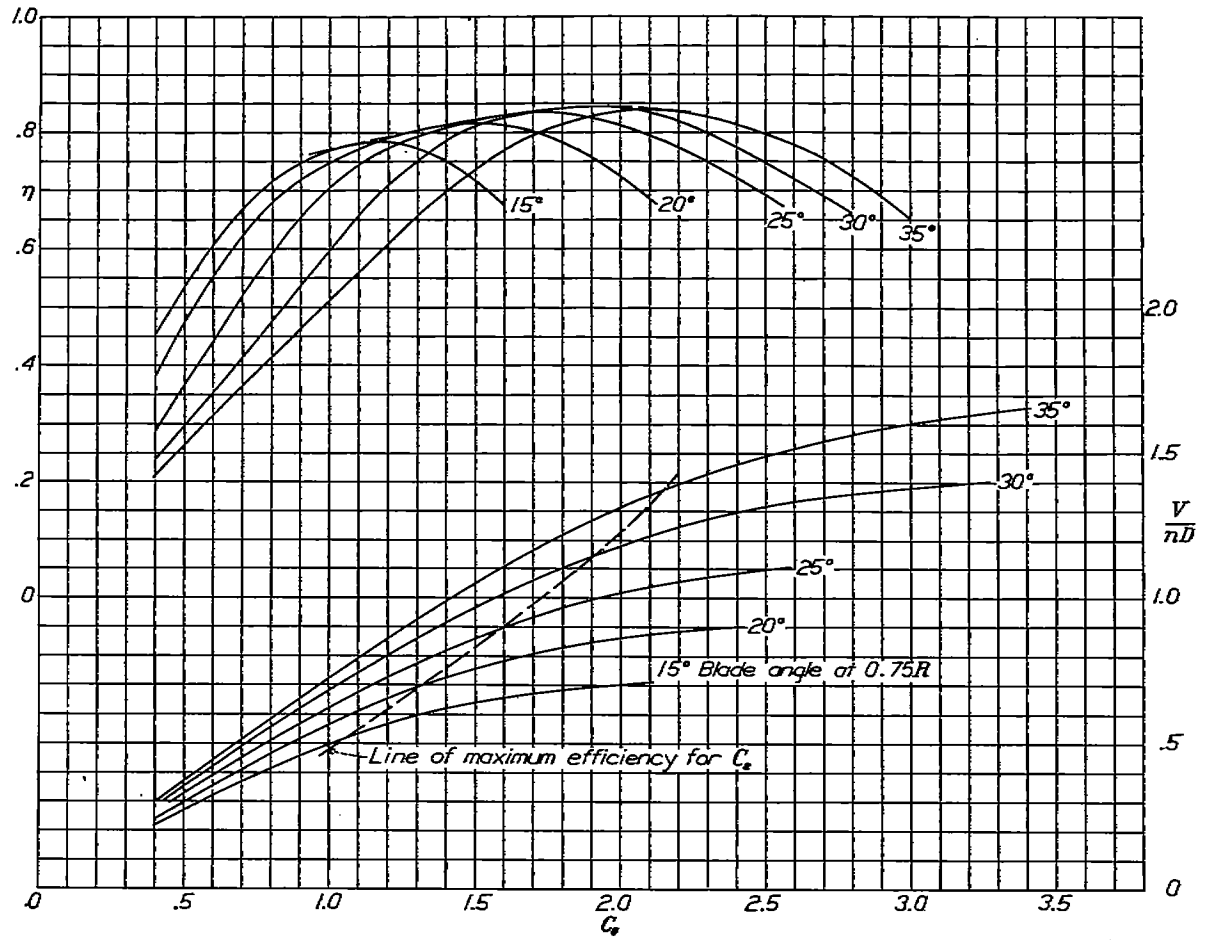

FIGURE 41.—Design chart for propeller 6131, 3 blades, liquid-cooled engine nacelle.

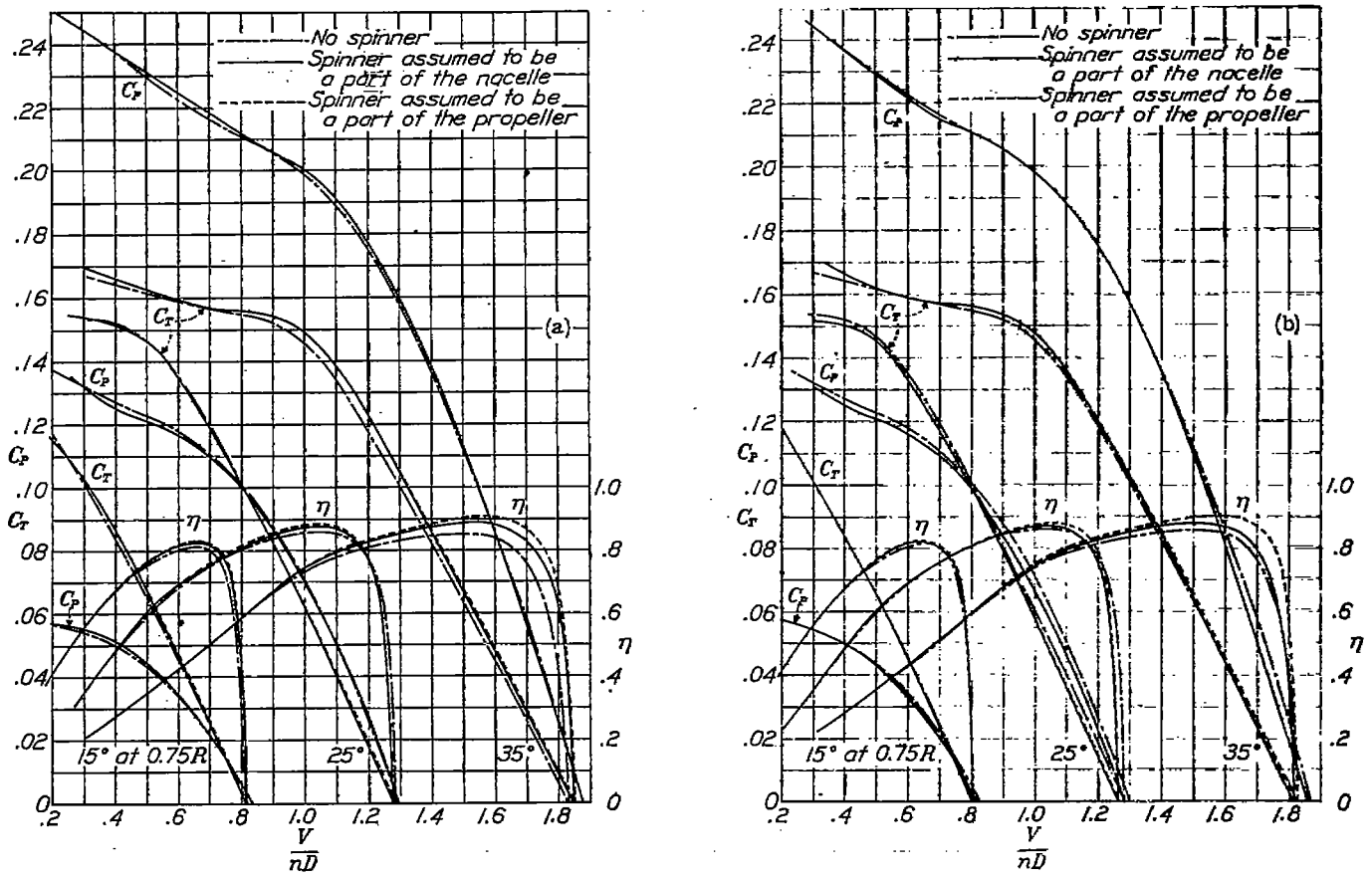

(a) Spinner 1. (b) Spinner 2.

FIGURE 42.—Effect of spinner on propeller characteristics. Propeller 5808-9, 3 blades, liquid-cooled engine nacelle.

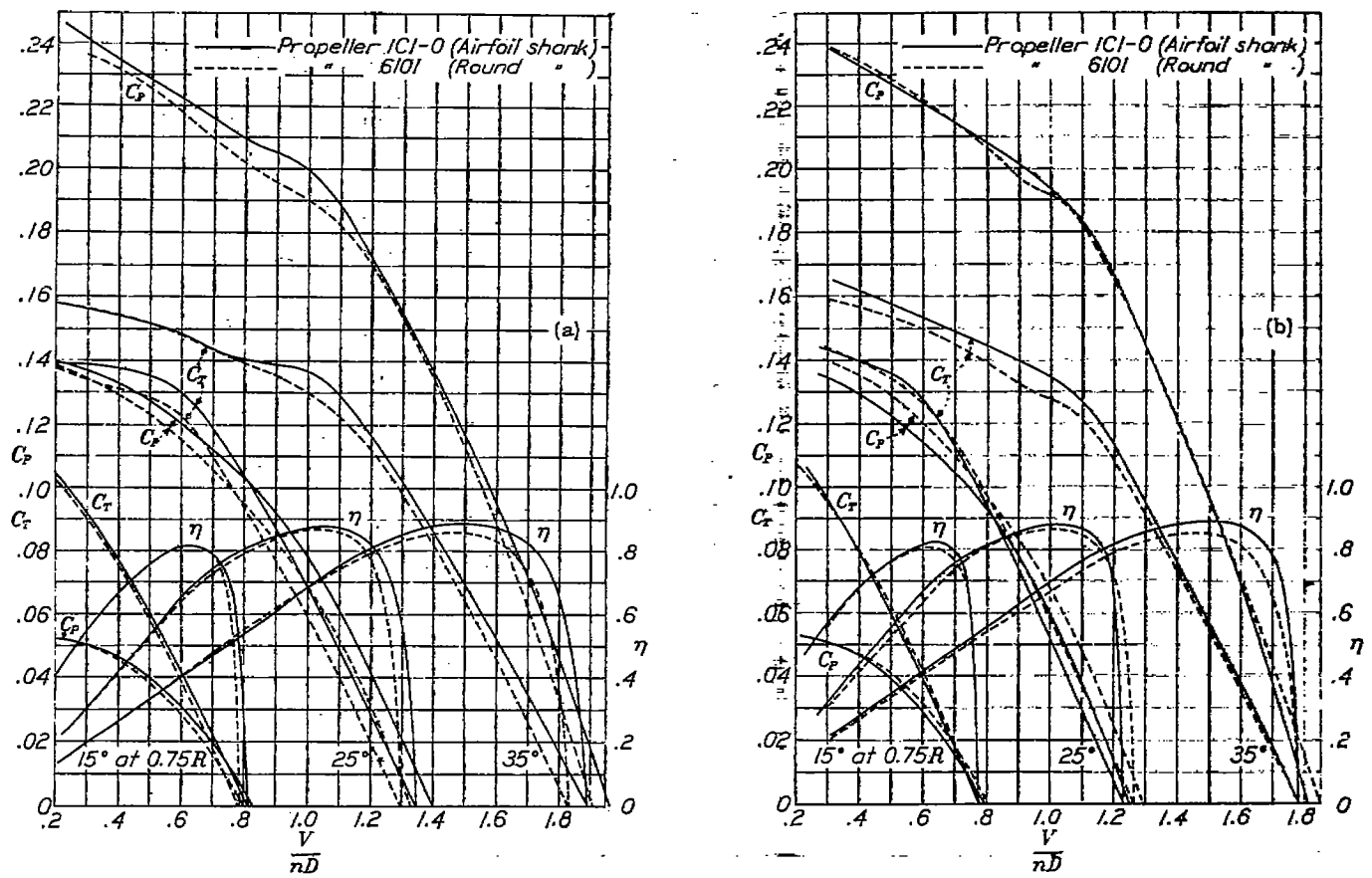

(a) Radia lengine nacelle. (b) Liquid-cooled engine nacelle.

FIGURE 43.—Comparison o itwo propellers having different blade-shank shapes.

Use of data.—The computation of thrust at all air speeds is facilitated through the use of lines of constant C_T superposed on the power curves. Thrust coefficients are also given in the usual type of plot. The use of the combined C_P and C_T curves is illustrated in the following outline:

Computation of thrust for a constant-speed controllable propeller:

1. Compute C_s from design conditions.
2. Determine V/nD from C_s chart.
3. Compute diameter from V/nD.
4. Solve for C_P, C_P=power/$\rho n^3 D^5$.
5. Determine C_T for several values of V/nD from the combined C_T and C_P curves. Follow the line of constant C_P.
6. Solve for thrust, $T=C_T\rho n^2 D^4$.
7. Solve for velocity from assumed V/nD.

Computation of thrust for a fixed-pitch propeller:

1. Compute C_s from design conditions.
2. Determine $(V/nD)_{max}$ and blade angle from C_s chart.
3. Solve for diameter from $(V/nD)_{max}$.
4. Solve for C_P for high speed $(C_{P_{max}})$.
5. Determine C_P and C_T for several values of V/nD from the combined C_T and C_P curves. Follow the line for constant blade angle.
6. Solve for N/N_{max} from relationship $N/N_{max}=\sqrt{C_{P_{max}}/C_P}$. (This relationship is based on the assumption that the torque is constant for small changes in engine speed for a constant throttle setting.)
7. Solve for V/V_{max} from the relationship $V/V_{max}=\frac{(V/nD)}{(V/nD)_{max}}\frac{N}{N_{max}}$
8. Compute thrust from $T=C_T\rho n^2 D^4$

$$=C_T\frac{C_{P_{max}}}{C_P}K$$

where $K=\rho n^2_{max} D^4$

n, propeller speed, r. p. s.
N, propeller speed, r. p. m.

Static thrust and power.—The static thrust and static power coefficients, obtained from the Wright Field tests of propellers 6101, 6129, and 6131 (reference 6) are shown (figs. 14, 16, 18, 20, 22, and 24) for the purpose of comparison. It may be noted that the Wright Field data check the present data closely for certain conditions and poorly for others. Particularly poor is the check for propeller 6131, for which there is a consistent difference of 15 to 20 percent. This lack of agreement is not particularly disturbing because there are several important differences in the method of testing. The whirl rig at Wright Field is in the open air and represents the same conditions as encountered with a stationary airplane on the ground. The forward speed is zero and the V/nD is consequently assumed to be zero; whereas, the slipstream of the propeller in a wind tunnel creates a circulation of air through the tunnel and the V/nD is computed from the measured velocity. The wind-tunnel results are extrapolated to zero V/nD. There is some question as to whether the assumed velocities are entirely comparable for the two conditions. Furthermore, the body conditions were different for the two tests. It is well known that large bodies slow up the air passing through the propeller disk, thus causing the propeller sections to operate at higher angles of attack. This effect is brought out clearly in the present report. Also, it is possible that the blade-angle setting for propeller 6131 was different for the two tests since the differences noted are consistent.

SPINNER RESULTS AND VARIOUS OTHER COMPARISONS

The material for this report was selected with the view to presenting information regarding the effect of current body styles on propeller characteristics as well as of presenting the actual propeller data. An important modification of the liquid-cooled engine nacelle is that of the spinner. Spinners were not tested on the radial engine nacelle because previous tests indicated no aerodynamic advantage. As the shape of the propeller-blade shank is closely allied to the subject of spinners, data for two shank shapes are included. An incidental comparison of blade-thickness effects is made because the results are of interest. A comparison is also made of three blade sections; this material is of an incidental nature because a separate report covers this subject (reference 4). The propellers for the two reports, however, are different.

Spinners.—The aerodynamic purpose of a spinner is to reduce the body drag, to reduce the drag of the hub and of the shank portions of the blades, and to reduce the engine torque required. In order to fulfill this purpose, the spinner should fair smoothly into the outlines of the body and yet enclose the hub and the round portions of the blade shanks. Two sizes of spinners were tested, both fairly large, as may be noted from figure 1. The results of the tests, given in curve form in figure 42, were computed on two bases: on one basis, the reduction in body drag due to the spinner is credited to the body and consequently does not show up in the propulsive efficiency; and, on the other basis, the reduction in body drag is credited to the propeller and shows up as a gain in propulsive efficiency. In the first case, the spinner is assumed to be a part of the body, the results being shown as solid lines; and, in the second, to be a part of the propeller, the results being shown as broken lines. Both methods, of course, show any gains in propulsive efficiency resulting from covering up the hub and shank portions of the blades.

An analytical summary of the results is given in the following table. Of interest is the fact that the smaller (spinner 1) of the two spinners is superior. Also, the advantage of spinner 1 increases with blade-angle setting, the gain in efficiency being only 1.5 percent for 15° and 6.0 percent for 35°. Of this 6.0 percent maximum

gain, 4 percent is due to covering up the hub and the shank portions of the blades and only 2 percent is due to reduced body drag.

The addition of streamline fairings over the shank portions of the blades, extending out from spinner 1

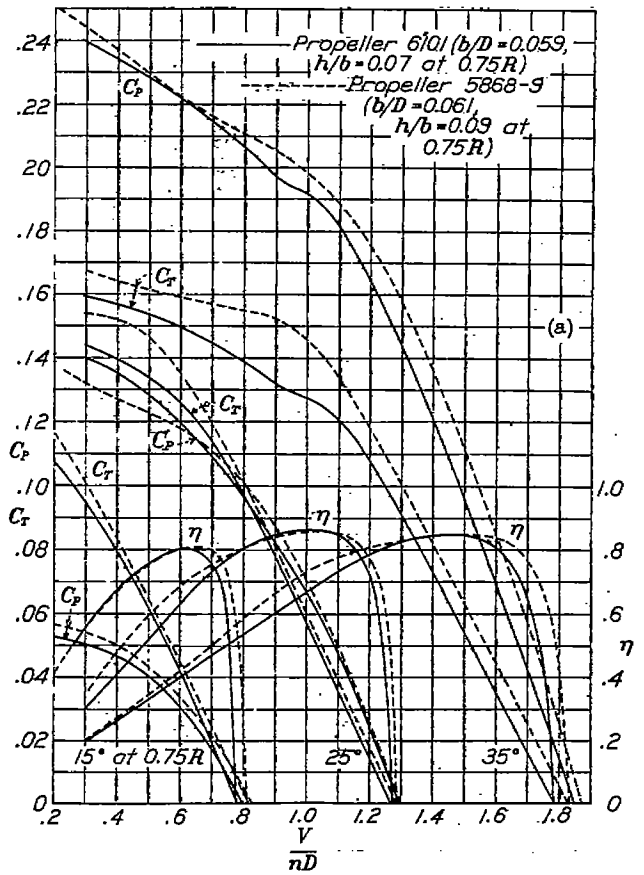

(a) Characteristic curves.

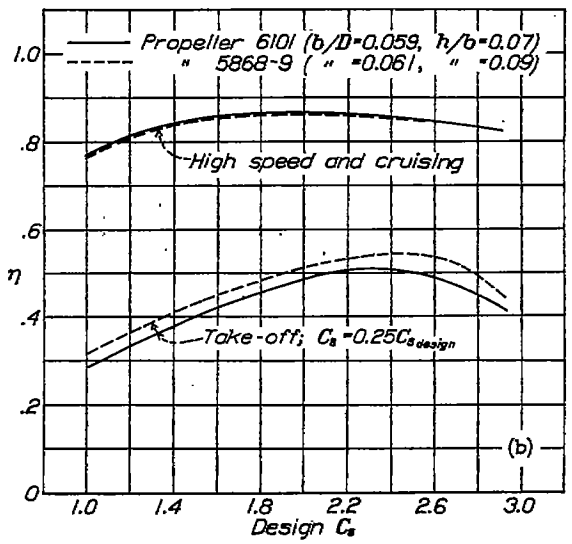

(b) Comparative performance computed for high-speed and take-off conditions for controllable operation.

FIGURE 44.—Comparison of two propellers differing essentially in thickness. Liquid-cooled engine nacelle.

a distance of about 4 inches (see fig. 5), increased the efficiency an additional 1 percent for the one blade-angle setting investigated, 25°. The value of 1 percent, however, is within the experimental error for this particular test.

SUMMARY OF RESULTS WITH SPINNERS

Cowling nose shape	Body drag at 100 m. p. h. (lb.)	η_a			η_b			Gain in η due to spinner [η_a (spinner)—η_a (no spinner)]			Gain in η due to lower body drag [η_b—η_a]			Total gain due to spinner [η_b (spinner)—η_b (no spinner)]		
	Blade angle →	15°	25°	35°	15°	25°	35°	15°	25°	35°	15°	25°	35°	15°	25°	35°
No spinner	59.0	81.5	86.5	85.0	81.5	86.5	85.0									
Spinner 1	57.0	82.5	87.5	89.0	83.0	88.5	91.0	1.0	1.0	4.0	0.5	1.0	2.0	1.5	2.0	6.0
Spinner 2	56.5	82.0	87.0	88.0	82.5	88.0	90.0	.5	.5	3.0	.5	1.0	2.0	1.0	1.5	5.0
Spinner 1 and cuffs	57.0		88.0			89.0			1.5			1.0			2.5	

Body drag includes support drag.
η_a is the efficiency computed using drag of body with spinner in place, spinner assumed to be a part of the body.
η_b is the efficiency computed using drag of body with no spinner (59 lb.), spinner assumed to be a part of the propeller.

Blade-shank shape.—Propeller 6101 has round shanks extending from the controllable hub for 6 or 8 inches before the transition from round to airfoil shape is well under way. Propeller 1C1–0 is of the same design, except that the airfoil shape is carried to within an inch or so of the adjustable hub.

The results of tests of these two propellers mounted on the radial engine nacelle (fig. 43 (a)) indicate an advantage in favor of propeller 1C1–0, particularly for the highest blade angles. A small difference in V/nD for zero thrust indicates that the airfoil shanks contribute to the thrust. The advantage of propeller 1C1–0 is greater for the liquid-cooled engine nacelle. (See fig. 43 (b).)

Blade thickness.—Propeller 5868–9 is about 29 percent thicker at the $0.75R$ station than propeller 6101. (This greater thickness means that the camber also is 29 percent higher for propeller 5868–9 than for propeller 6101.) The difference in width is unimportant since the magnitude is only about 3 percent. A comparison of these propellers tested in front of the liquid-cooled engine nacelle (fig. 44 (a)) reveals three interesting results: first, there is little or no difference in maximum efficiency; second, the thick propeller (5868–9) has an appreciably higher efficiency in the take-off and climbing range; and, third, there is a small difference in V/nD for zero thrust. The third point merely indicates that the thick propeller has the higher aerodynamic pitch, as would be expected.

A comparison of the propellers for the high-speed and the take-off conditions for controllable operation is given in figure 44 (b). This plot brings out the advantage of the thick propeller for take-off but there is an indication that some sacrifice, however small, is made at high speed. The apparent reason for the advantage of the thick propeller at low V/nD operation is the delayed stall of the sections resulting in a higher lift or thrust coefficient. (See fig. 44 (a).) This effect of thickness (or camber) is substantiated by more general tests reported in reference 7.

It may be well to point out here that thick propellers lose more in take-off efficiency owing to compressibility at high tip speeds than do thin ones. (See reference 1.) Compressibility effects will equalize the take-off efficiencies of propellers of different thickness when the tip speed is sufficiently high.

Blade section.—The relative merit of the different blade sections investigated is shown by figure 45. In figure 45 (a) a comparison is made for the cruising and the take-off conditions using the data for the radial engine nacelle. The order of decreasing merit of the sections for cruising is Clark Y, N. A. C. A. 2400–34, and R. A. F. 6. The difference between the first two sections is only about 1 percent, well within the experimental error, while the difference between the Clark Y and the R. A. F. 6 is between 2 and 4 percent. The efficiency of the R. A. F. 6 propeller is several percent higher than the Clark Y for the take-off condition and the Clark Y is likewise more efficient than the N. A. C. A. 2400–34. It may be seen, by reference to the basic data, that superior take-off characteristics are a result of a delayed stall and higher thrust coefficients.

It should be pointed out, also, that the R. A. F. 6 section is more sensitive to compressibility than the other two sections for the take-off condition; therefore the efficiencies tend to equalize as the tip speed is increased. (See reference 1.)

The relatively poor take-off characteristics of the propeller of N. A. C. A. 2400–34 section were expected for these low tip speeds because of the low maximum lift coefficient of the section. This section was developed for high tip speeds and should properly be used only for the tip sections, inasmuch as its principal merit is the later compressibility stall.

Figure 45 (b) shows the same comparisons and the same order of merit for the liquid-cooled engine nacelle as were shown for the radial engine nacelle. The cruising efficiency of propeller 6131 (N. A. C. A. 2400–34 section) seems low in comparison with propeller 6101 (Clark Y section), which suggests an error of 1 or 2 percent. The take-off efficiency of all three propellers tested with the liquid-cooled engine nacelle is consistently several percent higher than with the radial engine nacelle. This result is probably due to the influence of the body on the stalling of the blades. The radial engine body, being larger, slows the air and causes an earlier stall than the liquid-cooled engine body.

It should be pointed out that the foregoing comparisons were based on propellers of the same diameter for the same design condition. This basis was deemed better than any other since the take-off efficiency is very sensitive to changes in diameter whereas the design efficiency (high speed or cruising) is only slightly sensitive. Had the diameter been allowed to vary, depending upon the V/nD chosen for maximum efficiency, there would have been large differences in take-off efficiency due entirely to the differences in the diameters.

Body.—The relative effect of the two bodies on the characteristics of the five propellers tested is given by figure 46. The maximum efficiencies of each propeller appear to agree fairly closely for the two body conditions, with the exception of that for propeller 6131, which was previously mentioned as probably being slightly in error. There are two opposing factors that tend to keep the maximum efficiencies the same for the two

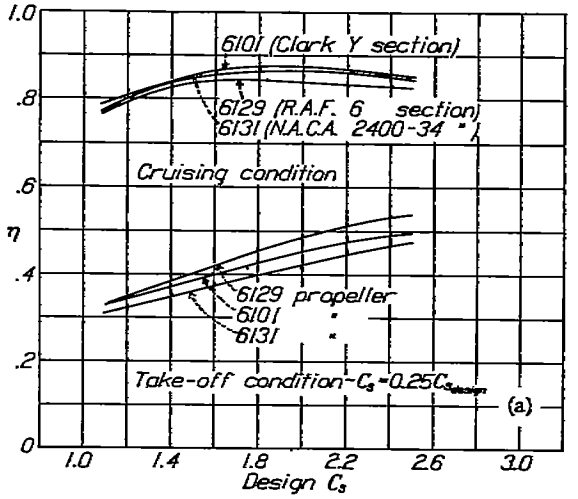

(a) Radial engine nacelle.

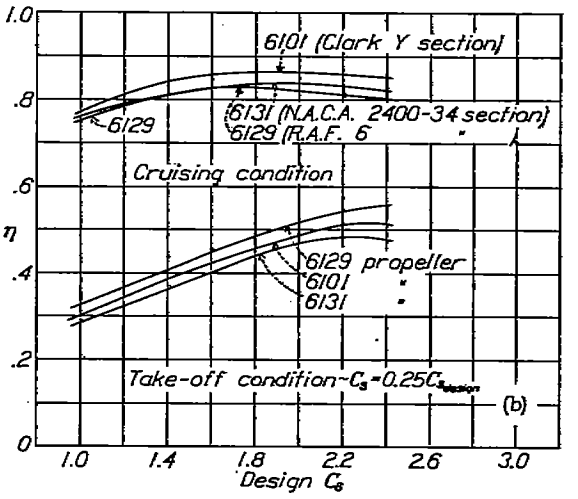

(b) Liquid-cooled engine nacelle.

FIGURE 45.—Comparison of three controllable propellers having different airfoil sections. All are the same diameter for the same C_s.

bodies. The slipstream drag, which reduces the efficiency, is greater for the radial engine nacelle than for the smaller liquid-cooled engine nacelle. On the other hand, the hub and blade shanks have less drag when they are located in front of the blunt nose of the radial engine nacelle than when they are located in front of the liquid-cooled engine nacelle. If a spinner had been used for all the tests of the liquid-cooled engine nacelle, it is clear that the peak efficiencies would have been higher than those for the radial engine nacelle. (See spinner results.)

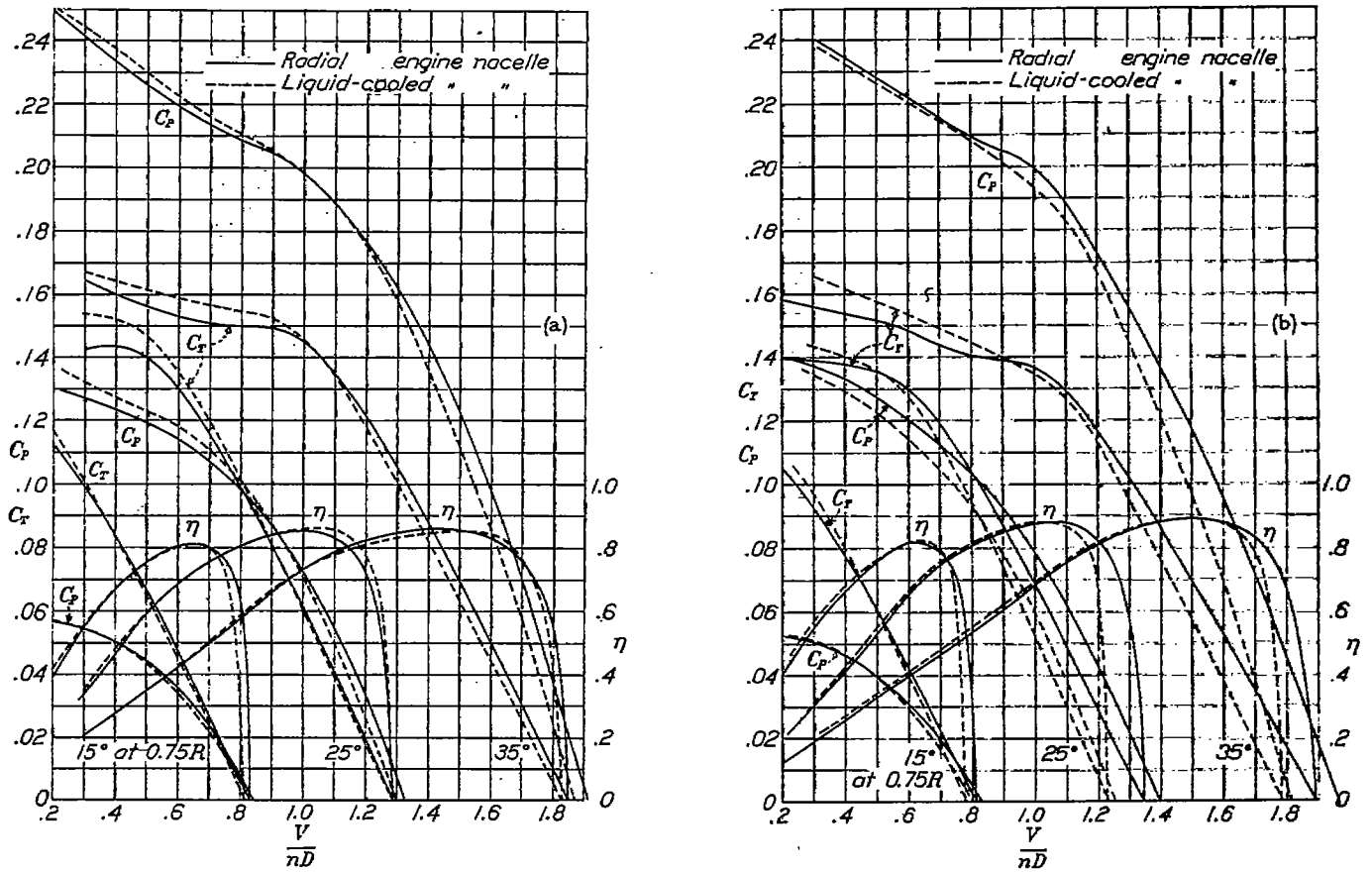

(a) Propeller 5868-9.

(b) Propeller 1C1-0.

(c) Propeller 6101.

(d) Propeller 6129.

FIGURE 46.—Comparison of propeller characteristics for two body conditions.

The take-off efficiencies are consistently higher for the liquid-cooled engine nacelle than for the other nacelle. It may be noted in every comparison (fig. 46) that the thrust curves for the liquid-cooled engine nacelle reach higher values of C_T at the take-off condition than for the radial engine nacelle. This effect results from a difference in air speed over the two bodies.

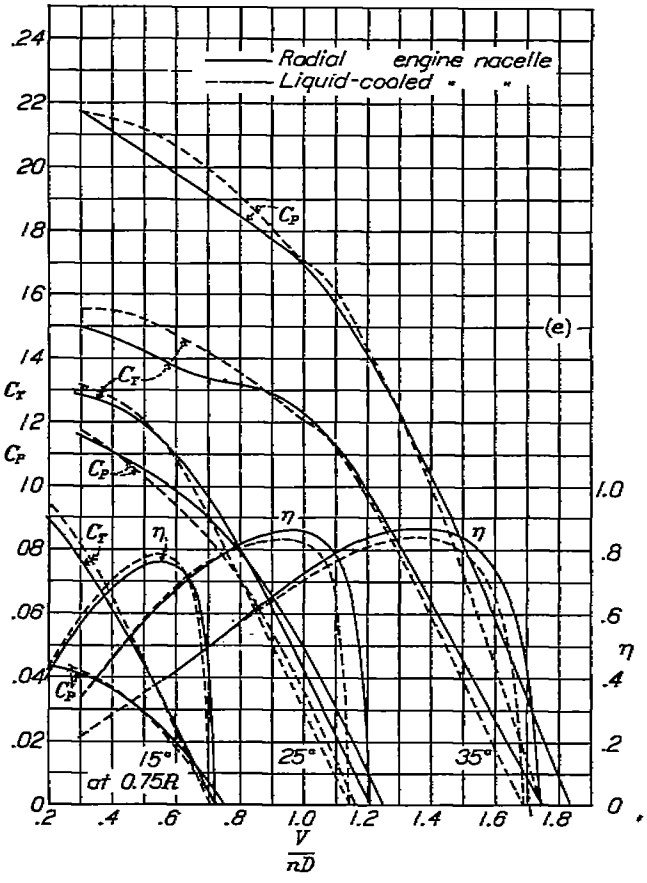

(e) Propeller 6131.

FIGURE 46.—Continued. Comparison of propeller characteristics for two body conditions.

The liquid-cooled engine nacelle slows down the air to a lesser extent than the larger radial engine nacelle and the blades do not stall so quickly at the low V/nD values. A rough estimate of the differences in mean air speed through the propeller disk for the two bodies can be made by computing the relative velocities for zero thrust. The greatest difference in velocity noted is for propeller 1C1–0 and amounts to about 7 percent.

CONCLUSIONS

The results of the tests made at moderately low tip speeds of five propellers indicated the following conclusions:

1. Propellers operated in front of the liquid-cooled engine nacelle had higher take-off propulsive efficiencies than when operated in front of the radial engine nacelle; they also had higher cruising efficiencies when provided with suitable spinners.

2. Spinners mounted on the liquid-cooled engine nacelle not only reduced the drag of the body but reduced the drag of the propeller hub and shanks as well. The propulsive efficiency was increased a maximum of 6 percent for one condition.

3. A propeller with airfoil sections extending into the hub was more efficient than one having round blade shanks when tested in front of both the radial and the liquid-cooled engine nacelles.

4. A thick propeller having a Clark Y section was found to be more efficient than a thin one for the take-off condition, but the maximum efficiency was possibly slightly less.

5. The order of decreasing efficiencies for the cruising condition for propeller-blade sections of 0.07 thickness ratios at $0.75R$ was found to be: Clark Y, N. A. C. A. 2400–34, and R. A. F. 6, but the order changed to R. A. F. 6, Clark Y, and N. A. C. A. 2400–34 for the take-off condition for propellers of the same diameter.

LANGLEY MEMORIAL AERONAUTICAL LABORATORY,
NATIONAL ADVISORY COMMITTEE FOR AERONAUTICS,
LANGLEY FIELD, VA., *November 23, 1937.*

REFERENCES

1. Biermann, David, and Hartman, Edwin P.: The Effect of Compressibility on Eight Full-Scale Propellers Operating in the Take-Off and Climbing Range. T. R. No. 639, N. A. C. A., 1938.
2. Hartman, Edwin P., and Biermann, David: The Aerodynamic Characteristics of Full-Scale Propellers Having 2, 3, and 4 Blades of Clark Y and R. A. F. 6 Airfoil Sections. T. R. No. 640, N. A. C. A., 1938.
3. Hartman, Edwin P., and Biermann. David: The Negative Thrust and Torque of Several Full-Scale Propellers and Their Application to Various Flight Problems. T. R. No. 641, N. A. C. A., 1938.
4. Biermann, David, and Hartman, Edwin P.: The Aerodynamic Characteristics of Six Full-Scale Propellers Having Different Airfoil Sections. T. R. No. 650, N. A. C. A., 1939.
5. Weick, Fred E., and Wood, Donald H.: The Twenty-Foot Propeller Research Tunnel of the National Advisory Committee for Aeronautics. T. R. No. 300, N. A. C. A., 1928.
6. Enos, L. H., and Sims, J. A.: Static Thrust Characteristics of Propellers Using Clark Y, R. A. F. 6, and 2400 Profiles. A. C. T. R. Serial No. 4319, Matériel Division, Army Air Corps, 1937.
7. Freeman, Hugh B.: Comparison of Full-Scale Propellers Having R. A. F. 6 and Clark Y Airfoil Sections. T. R. No. 378, N. A. C. A., 1931.